

ARCHAEOMETRICAL INVESTIGATION OF SOME GLASS
SAMPLES FROM MERSİN OLBA ARCHAEOLOGICAL SITE

A THESIS SUBMITTED TO
THE GRADUATE SCHOOL OF NATURAL AND APPLIED SCIENCES
OF
MIDDLE EAST TECHNICAL UNIVERSITY

BY

CEM DOĞAN

IN PARTIAL FULFILLMENT OF THE REQUIREMENTS
FOR
THE DEGREE OF MASTER OF SCIENCE
IN
ARCHAEOMETRY

SEPTEMBER 2014

Approval of the thesis:

**ARCHAEOMETRICAL INVESTIGATION OF SOME GLASS
SAMPLES FROM MERSİN OLBA ARCHAEOLOGICAL SITE**

submitted by **CEM DOĞAN** in partial fulfillment of the requirements for the degree
of **Master of Science in Archaeometry Department**, Middle East Technical
University by,

Prof. Dr. Canan Özgen
Dean, Graduate School of **Natural and Applied Sciences**

Prof. Dr. Ümit M. Atalay
Head of Department, **Archaeometry**

Assoc. Prof. Dr. Gülay Ertaş
Supervisor, **Chemistry Dept., METU**

Assistant Prof. Dr. Ali Akın AKYOL
Co-Supervisor, **Cons. and Rest. of Cultural Properties Dept., Gazi University**

Examining Committee Members:

Prof. Dr. Asuman Türkmenoğlu
Geological Engineering Dept., METU

Assoc. Prof. Dr. Gülay Ertaş
Chemistry Dept., METU

Prof. Dr. Emel Erten
Archaeology Dept., Gazi University

Prof. Dr. Burcu Erciyas
Settlement Archaeology Dept., METU

Assistant Prof. Dr. Ali Akın Akyol
Cons. & Rest. of Cult. Properties Dept., Gazi University

Date: 15 September 2014.

I hereby declare that all information in this document has been obtained and presented in accordance with academic rules and ethical conduct. I also declare that, as required by these rules and conduct, I have fully cited and referenced all materials and results that are not original to this work.

Name, Last Name : Cem, Dođan

Signature :

ABSTRACT

ARCHAOMETRICAL INVESTIGATION OF SOME GLASS SAMPLES FROM MERSİN OLBA ARCHAEOLOGICAL SITE

Dođan, Cem

M.S., Graduate Program of Archaeometry

Supervisor: Assoc. Prof. Dr. Glay Ertař

Co-Supervisor: Assistant Prof. Dr. Ali A. Akyol

September 2014, 72 pages

Olba archaeological site is located in Mersin, Turkey. It is one of the most important regions of Rough Cilicia. We performed the analyses of 34 glass objects (IV. and VII. centuries C.E.) from Olba archaeological site using PED-XRF and Raman spectroscopy techniques. XRF and Raman spectroscopy results are mostly compatible with each other. The chemical compositions of the Olba glass samples are similar to each other and the results showed that the glasses are all soda-lime-silica based glasses. Additionally, for the production of the Olba glasses, soda was used as the fluxing agent and the main stabilizer was lime. SiO_2 , Al_2O_3 and Na_2O levels of Olba glass samples are relatively lower than typical soda-lime-silica glasses reported in the literature. Raman analyses results revealed that the Olba glasses were fired at temperatures above 1000°C according to their I_p values found to be higher than 1.

Keywords: Ancient Glass, Raman Spectroscopy, XRF, Archaeometry, Olba

ÖZ

MERSİN OLBA ARKEOLOJİK ALANI CAM BULUNTULARININ ARKEOMETRİK YÖNTEMLERLE İNCELENMESİ

Doğan, Cem

M.S., Graduate Program of Archaeometry

Tez Yöneticisi: Doç. Dr. Gülay Ertaş

Ortak Tez Yöneticisi: Yrd. Doç. Dr. Ali A. Akyol

Eylül 2014, 72 sayfa

Olba arkeolojik alanı Mersin ili sınırları içinde Türkiye’de yer alır. Olba, “Rough Cilicia”nın en önemli bölgelerinden biridir. Çalışma Olba arkeolojik alanından çıkartılan 34 adet cam objenin (M.S. IV ila VII. yy.) PED-XRF ve Raman Spektroskopisi teknikleri ile incelenmesi suretiyle gerçekleştirilmiştir. XRF ve Raman spektroskopisi tekniklerinden elde edilen sonuçlar genel itibariyle birbirleriyle uyumludur. Çalışma sonucunda Olba cam buluntularının kimyasal kompozisyonlarının benzer olduğu ve tüm cam buluntuların soda-kireç-silis camı olduğu değerlendirilmiştir. Raman spektroskopisinden alınan sonuçlar XRF sonuçları ile uyumludur. Olba camlarının üretiminde temel eritici olarak Soda ve sağlamlaştırıcı olarak da kireç kullanılmıştır. Olba cam örneklerinin SiO_2 , Al_2O_3 ve Na_2O seviyeleri, literatürde antik soda-kireç-silis camlarına atfedilen değerlerinden görece düşüktür. Raman analizi sonuçlarına göre, I_p değerleri “1”in üzerinde hesaplanan Olba cam örneklerinin 1000C° üzerinde eritildikleri anlaşılmaktadır.

Anahtar Kelimeler: Antik Cam, Raman Spektroskopisi, Arkeometri, Olba

ACKNOWLEDGMENTS

I would like to express my gratitude to Assoc. Prof. Dr. Glay Ertař, and Assist. Prof. Dr. Ali Akın Akyol as supervisor and co supervisors of the thesis.

I really would like to express my gratefulness to Prof. Dr. Emel Erten for providing the samples.

I owe very special thanks to Material Conservation Laboratory at the Faculty of Architecture at METU and Prof. Dr. Emine Caner Saltık for Raman analysis.

I am very grateful to Prof. Dr. Yusuf Kaęan Kadioęlu at the Department of Geological Engineering and Earth Sciences Application and Research Center (YEBİM) at Ankara University for XRF analysis.

Special thanks to Glřen Albuz for her kind support.

Finally, very special thanks to Prof. Dr. řahinde Demirci and Prof. Dr. Ay Melek zer and Prof. Dr. Yavuz Ataman for their continuous support.

TABLE OF CONTENTS

ABSTRACT	v
ÖZ.....	vi
ACKNOWLEDGMENTS.....	vii
LIST OF TABLES	x
LIST OF FIGURES.....	xi
CHAPTER 1.....	1
<u>1. INTRODUCTION</u>	1
1.1 Raman Scattering.....	2
1.2. Raman Spectroscopy of Silicate Glass	4
1.2.1 Q _n Model and Polymerization Index.....	5
1.2.2 Analysis of Ancient Glass and Glazes by Raman Spectroscopy	6
1.3. The Aim and Scope of the Study.....	9
<u>2. THE NATURE OF GLASS AND ITS HISTORY</u>	11
2.1 The Definition of Glass and Ancient Glass	11
2.2. Silicate Glasses	12
2.3. Raw Materials of Ancient Glass	14
2.4. A Brief History of Ancient Glass from the Very First Glass to Roman Glass	18
2.4.1. Glass from Beginning to the Roman Period	18
2.4.2. Roman Glass	20
2.5 Olba Archaeological Site.....	22
<u>3. MATERIALS AND METHODS</u>	24
3.1. Glass Samples Excavated from Olba Archaeological Site.....	24
3.2. Raman Spectroscopic Analysis of the Samples.....	26
3.3. X-Ray Fluorescence (XRF) Analysis of Glass Samples	28
<u>4. RESULTS AND DISCUSSION</u>	29
4.1. XRF Analysis of the Olba Glass Samples	29
4.2. Raman Spectroscopic Analysis of Olba Glass Samples.....	37
<u>5. CONCLUSION</u>	51

REFERENCES.....	53
APPENDICES	
APPENDIX A. OPTICAL IMAGES OF THE OLBA GLASS SAMPLES	61
APPENDIX B THICKNESSES OF THE OLBA GLASS SAMPLES.	67
APPENDIX C. ELEMENTAL COMPOSITIONS OF THE OLBA GLASS SAMPLES.....	69

LIST OF TABLES

TABLES

Table 1. Chemical Classification of Glasses.....	12
Table 2. The average composition of some groups of glass found in wrecks.....	17
Table 3. Information on archaeological context of Olba glass samples.....	24
Table 4. Literature data, regarding the assigned wavenumbers for 5 components.	27
Table 5. Percent composition of the Olba glass samples.	30
Table 6. Percent composition of the Olba glass samples and LOI values.	31
Table 7. Average percent composition of the Olba glass samples.	32
Table 8. Peak maxima values of Si-O bending (Q_{Bmax}), stretching (Q_{Smax}) peaks and I_p indexes of the 32 Olba glass samples.	41
Table 9. Band positions and assignments of the various peaks within the Olba glass composition.	47
Table 10. Correlation between Fe_2O_3 , Na_2O , Al_2O_3 , SiO_2 concentration and Q_{B2} values.....	48

LIST OF FIGURES

FIGURES

Figure 1. The schematic illustration of Rayleigh scattering as well as Stokes and anti-Stokes Raman scattering.	3
Figure 2. Generalized Raman spectrum.	4
Figure 3. Qn Notation Model	5
Figure 4. SiO ₄ Tetrahedral Unit).....	13
Figure 5. Tetrahedra network structures of a) crystalline vs. b) amorphous SiO ₂ phases.	14
Figure 6. Cicilia and Olba region.	23
Figure 7. The scatter plot of TiO ₂ concentration vs. Fe ₂ O ₃ concentration of 34 Olba glass samples.	32
Figure 8. The scatter plot of SiO ₂ concentration vs. Fe ₂ O ₃ concentration of 34 Olba glass samples.	33
Figure 9. The scatter plot of Al ₂ O ₃ concentration vs. Fe ₂ O ₃ concentration of 34 Olba glass samples.	34
Figure 10. The scatter plot of Al ₂ O ₃ concentration versus SiO ₂ concentration of 34 Olba glass samples.	34
Figure 11. The scatter plot of Al ₂ O ₃ concentration versus CaO concentration of 34 Olba glass samples.	35
Figure 12. The scatter plot of Fe ₂ O ₃ concentration vs. MnO concentration of 34 Olba glass samples.	37
Figure 13. Raw Raman spectra of glass samples, 19ba, 79a, and 15ba.	38
Figure 14. Baseline corrected Raman spectra of glass samples, 19ba, 79a, and 15ba.	38
Figure 15. Raw Raman spectra of glass samples, 63ca, 33b, 59b.	39
Figure 16. Baseline corrected Raman spectra of glass samples, 63ca, 33b, 59b.	39
Figure 17. Deconvoluted Raman spectra of glass samples 15b, 19b, 79, 33, 59b, and 63c.	40

Figure 18. Classification of a variety of historical/ancient glasses using SiO₄ bending and stretching modes. Olba glass results are also shown in yellow color. Adapted from “A Raman spectroscopic study of glass trade beads excavated at Mapungubwe hill and K2” by Colomban et al., 2011..... 42

Figure 19. Polymerization index, I_p, vs. SiO₄ bending mode graph of various glass samples from the literature plus Olba glass samples. Adapted from “On-site Raman identification and dating of ancient/modern stained glasses at the Sainte-Chapelle, Paris.” by Colomban et al., 2007..... 43

Figure 20 Representative examples of *seven glass families*. Polymerization index, glass type and stretching modes are indicated. 44

Figure 21. SiO₄ stretching mode vs. polymerization index, I_p, plot of a wide variety of glasses plus Olba glass samples. Adapted from “On-site Raman identification and dating of ancient/modern stained glasses at the Sainte-Chapelle, Paris.” by Colomban et al., 2007. 45

Figure 22 Classification of window glass fragments based on their major composition. 46

Figure 23. Q_{B2} values vs. Fe₂O₃ concentration of the Olba glass samples. 48

Figure 24. The scatter plot of I_p index vs. Pb concentration of 32 Olba glass samples. 49

Figure 25. The scatter plot of Pb concentration vs. MnO concentration of 34 Olba glass samples. 50

CHAPTER 1

INTRODUCTION

Various analytical techniques are used to get objective evidence regarding the chemical and physical nature of excavated objects. These objects generally have unusual characteristics. Most importantly, they are irreproducible and exhaustible. In some cases, the material could be associated with an object which shall not be moved from its original place. In some other cases, physical integrity of the object can be extremely important as in the analyses of a valuable painting. Even if a sample from the object could be obtained and transferred from its original site to the laboratory, destruction of the sample is never preferable.

X-Ray based methods like XRF (X-ray Fluorescence) and XRD (X-ray Diffraction), Electron Microscopy techniques like SEM (Scanning Electron Microscopy), Ion-Beam Analysis techniques such as PIXE (Particle Induced X-ray Emission) and PIGE (Particle Induced Gamma Emission), Neutron Activation Analysis, Laser Ablation Inductively Coupled Plasma Mass Spectrometry, Infrared Spectroscopy Raman spectroscopy are some techniques used to analyze ancient glasses. Some of these techniques are non-destructive and can provide in-situ analyses (Edwards & Vandenabeele, 2012).

Recently, portable Raman spectrometers which have been designed to be carried frequently or even smaller as to fit into the palm of one hand are commercially available. In situ applications without necessity of moving the object from its original location are also possible by this method. Provided that usage of convenient laser power specific to the sample, Raman spectroscopy is undoubtedly a beneficial

molecular technique for the non-destructive analysis of ancient and historical materials (Vandenabeele, Edwards, & Jehlicka, 2014).

1.1 Raman Scattering

The phenomenon of inelastic scattering of the light hypothesized by Smekal in 1923, not long after in 1928 it is observed experimentally first by Raman and Krishnan (Dent, 2005). Chandrasekhara Venkata Raman (1888-1970) was awarded the Nobel Prize in physics in 1930 after his discovery of Raman phenomenon.

“Raman scattering is used to obtain information about the structure and properties of the molecules from their vibrational transitions” (Lewis & Edwards, 2001). Elastic and inelastic scattering are two types of scattering processes observed when light is scattered from a molecule: In elastic scattering process, the scattered photons have the same energy as the incident ones. These elastically scattered photons are called as Rayleigh scattering photons. Additionally, a small number of photons are scattered inelastically having different energy than the incident photons. Inelastic scattering process is called Raman scattering. The molecule should be excited from the ground state to a virtual energy state, and then relax into an excited vibration state, which generates Stokes Raman scattering in order to obtain the Raman effect. However, the molecule can stay in a higher vibrational energy state, in this case the Raman scattering is then called anti-Stokes Raman scattering. Stokes scattering occurs at lower energy than the Rayleigh scattering, and anti-Stokes radiation has greater energy, while both Stokes and anti-Stokes are equally displaced from the Rayleigh feature as shown in Figure 1. Usually, Stokes scattering is followed in Raman Spectroscopy since anti-Stokes scattering is less intense. Raman scattering via this virtual state can be thought as the polarization of the molecules electron cloud. The electric field of the incident light will force the electron cloud surrounding the molecule to oscillate with illumination. The oscillating electrons will then radiate an optical field which is identical to that of the incident light. The electron cloud is symmetrically distributed around a single atom and thus the re-radiated light is equally probable in any in-plane direction and will be in the same frequency as the

incident light, this is called Rayleigh scattering. The electron cloud surrounding the molecule will oscillate at the frequency of the incident light, but the absolute shape of the cloud will change at the frequency of the molecular vibrations. This oscillation in the shape of the electron cloud will subsequently change the optical field generated. A Fourier analysis of the scattered light will contain frequency components equal to the incident light, as well as other frequencies both higher and lower than the incident light. In addition, if the molecule is not vibrating, at any given moment in time the electron cloud will form a dipole moment across the atoms. Different atoms will feel a different field and so a different force will be applied to each atom. This is sufficient to induce a vibrational mode within the detection tool in various applications, but also generates a stimulus for the study of the interfacial processes involving enhanced optical scattering from adsorbates on metal surfaces. It is a breakthrough that the employment of surface enhancement has solved the low intensity problem of Raman scattering and made it possible to work as a more satisfying surface technique.

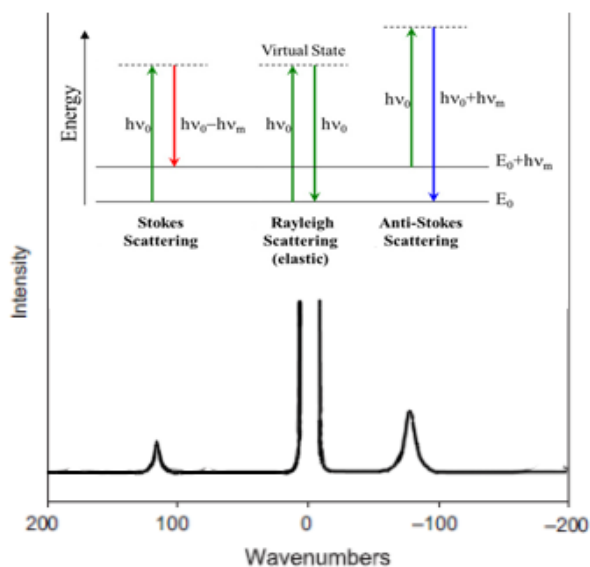


Figure 1. The schematic illustration of Rayleigh scattering as well as Stokes and anti-Stokes Raman scattering.

Plot of the intensity of radiation against the wavenumber difference between the source and the scattered energy gives the Raman spectra. Raman spectra can display

three types of radiation: Rayleigh scattering, Stokes lines, and anti-Stokes lines as shown in Figure 2.

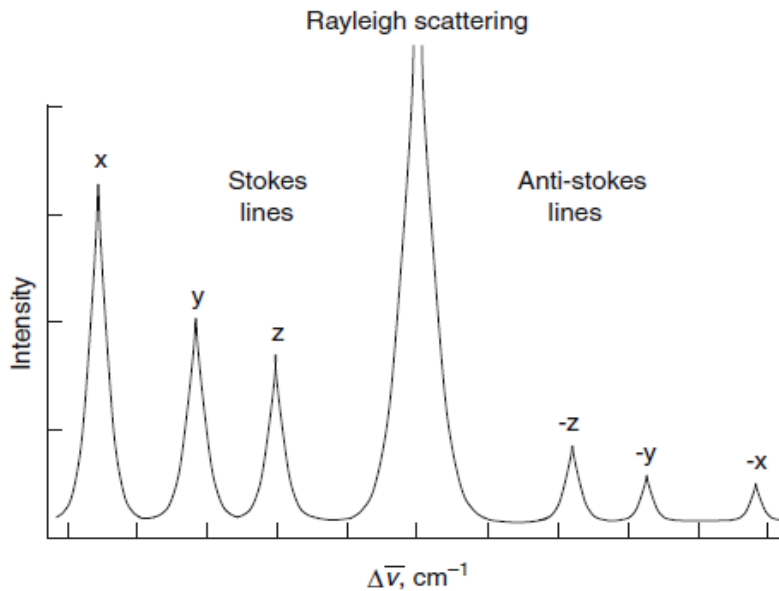


Figure 2. Generalized Raman spectrum (Larkin, 2011).

1.2. Raman Spectroscopy of Silicate Glass

Glass structure is a network of SiO_4 tetrahedral units linked to each other by sharing their oxygen atoms. Addition of fluxing agents to lower the melting temperature of pure α -quartz glass cause to the modification of Si-O network by replacing Si^{4+} covalently bonded atoms by non-covalent bonded atoms. Connectivity of Si-O network is decreased with this modification.

In a typical Raman spectrum of silicate two parts can be distinguished related to the molecular signature of SiO_4 . Two broad bands around 500 and 1000 cm^{-1} compose a typical molecular signature of silica glass. While the band around 1000 cm^{-1} is reflecting *stretching vibration* of SiO_4 tetrahedra, 500 cm^{-1} band reflects *bending vibration* mode (Philippe Colomban, 2003b; Philippe Colomban, Tournie, et al., 2006).

1.2.1 Q_n Model and Polymerization Index

Modification of Si-O network by atoms such as Na, K, Ca and Pb make changes in positions, intensity and shape of Raman signatures of silicate glass. Q_n notation model which is used to explain those changes in silicate network uses SiO_4 tetrahedron as the vibrational unit (Figure 3). A tetrahedron sharing all four oxygen atoms is designated as (Q_4). While isolated tetrahedron with no bridging (shared) oxygen atom is designated as (Q_0), tetrahedra linked by a common oxygen atom is designated as (Q_1), tetrahedra linked by sharing two and three oxygen atoms are designated as (Q_2) and (Q_3) (Janssens, 2013).

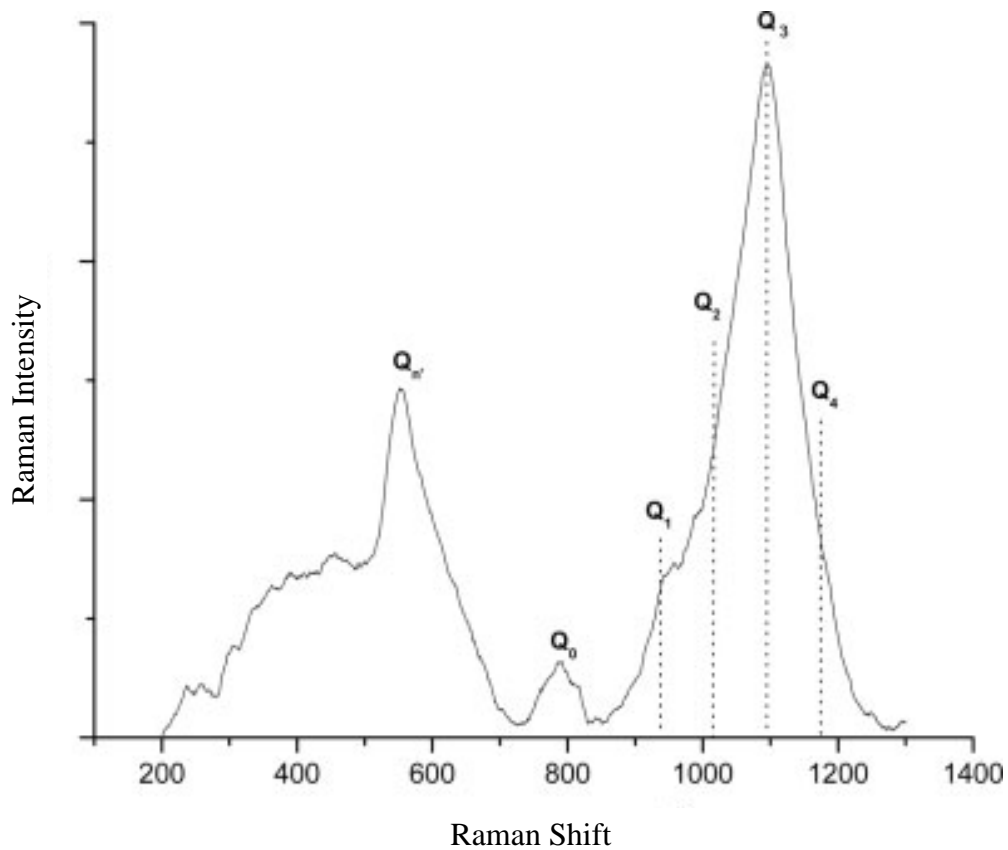


Figure 3. Q_n Notation Model (Baert et al., 2011).

The ratio of the area of the Si-O bending modes (A_{500}) vs. the area of the Si-O stretching modes (A_{1000}) gives the polymerization index I_p . There is a strong correlation between the polymerization degree of glass and the glass nanostructure,

composition and melting temperature (P. Colomban & Slodczyk, 2009). I_p index also can be used as a tool to characterize the glass in combination with the parameters of the Q_n model, namely the wavenumbers and area of each Q_n component (Janssens, 2013).

1.2.2 Analysis of Ancient Glass and Glazes by Raman Spectroscopy

The earliest example of the use of Raman spectroscopy for the characterization of historical silica material is the study of Brooke et al. (Brooke, Edwards, & Tait, 1999) on samples of broken underglaze blue terracotta tiles. The main aim of the study has been the analysis of post-medieval pigments. A study of the identification of the microstructure and compositions of the components of some ancient Vietnamese porcelains was also one of the first application of Raman spectroscopy on glazes (Nguyen Quang Liem, 2000). In this study it was demonstrated that Raman spectra of glaze could be obtained without preparation of the samples. In another study, non-destructive Raman spectroscopy was used to identify the different porcelains of French Royal manufacture (Ph Colomban & Treppoz, 2001; Philippe Colomban, Sagon, & Faurel, 2001). These studies were examples of the use of Si–O stretching components to distinguish different glazes from each other such as lead-based and alkali-based glazes. Afterwards, a number of ancient objects for instance pottery enamels, beads, rings, mosaics tesserae and porcelain glazes from different origins were examined by Philippe Colomban and his coworkers (Ph Colomban, 2004; Ph Colomban & Treppoz, 2001; Philippe Colomban, 2003a, 2003b, 2008; Philippe Colomban, Etcheverry, Asquier, Bounichou, & Tournié, 2006; Philippe Colomban, Milande, & Le Bihan, 2004; Philippe Colomban & Paulsen, 2005; Philippe Colomban et al., 2001; Philippe Colomban, Tournie, & Ricciardi, 2009; Philippe Colomban & Tournié, 2007; Philippe Colomban, Tournie, et al., 2006; Nguyen Quang Liem, 2000; Prinsloo, Tournié, & Colomban, 2011; Raškovska, Minčeva-Šukarova, Grupče, & Colomban, 2009; Ricciardi, Colomban, Tournié, & Milande, 2009; Simsek, Colomban, & Milande, 2009; Tanevska, Colomban, Minčeva-Šukarova, & Grupče, 2009; Tournié, Prinsloo, & Colomban, 2012). Modern porcelain enamels are used as compositional references and through this

examination a Raman procedure is proposed (Philippe Colomban, 2003b). In this procedure, relation between addition of network modifiers, degree of polymerization and relative intensity of Si-O bending and stretching modes were described. Correlation of the ratio of bending and stretching envelopes and glass structure and firing technology were also demonstrated. Most importantly, seven glass families are identified with the help of the collected data. A small set of İznik ceramics was the focus of another study that has confirmed the potential of Raman spectroscopy as a non-destructive tool to classify glass samples (Philippe Colomban et al., 2004). Another study on selected glasses and glazes of a variety of origins, identification and classification of amorphous and coloring phases were conducted (Ph Colomban, 2004). Technology of glassmaking was the main focus of another study on Roman mosaic tesserae (Galli, Mastelloni, Ponterio, Sabatino, & Triscari, 2004). In a subsequent study, the method proposed by Colomban was applied to various ancient ceramic glazes and glasses that are representative of different production origins to firstly attempt to establish the relationship between the glaze composition and the Raman spectra (Philippe Colomban & Paulsen, 2005). Later on, attention of scholars attracted by stained glass with the purpose of on-site identification of stained-glass windows and their deterioration level and nanostructure changes (Bouchard, Smith, & Carabatos-Nedelec, 2007; Philippe Colomban, Etcheverry, et al., 2006; Philippe Colomban et al., 2009; Philippe Colomban & Tournié, 2007). In another study, search of the capability of Raman spectroscopy in differentiation of stable and unstable glasses was the main purpose (Robinet, Coupry, Eremin, & Hall, 2006) and it was stated that Raman spectroscopy is a practical tool to examine the stability of glass. Ricci et al. (Ricci, Miliani, Rosi, Brunetti, & Sgamellotti, 2007) conducted an experimental study on tin-opacified glasses to characterize processing techniques of glasses. Studies regarding the alteration of glass is carried out on historical soda silicate glasses in the collections of the National Museums of Scotland (Robinet, Eremin, Coupry, Hall, & Lacombe, 2007; Robinet, Hall, Eremin, Fearn, & Tate, 2009) and Raman spectroscopy is used to examine the origin of alteration. Successively, micro Raman spectroscopy was used to analyze ancient coloured glass beads from Sri Lanka for the identification of inorganic pigments used (Welter, Schüssler, &

Kiefer, 2007). Colombar's method was used to examine fragmented ancient beads recovered from Rhodes by Oikonomou et al. (Oikonomou, Triantafyllidis, Beltsios, Zacharias, & Karakassides, 2008) for the purpose of assessment of processing temperatures. Aside from the studies on stained window glasses, researches on Roman window glasses were performed in order to determine the chemical structure and production techniques (Baert et al., 2011; Raffaëly, Champagnon, Ollier, & Foy, 2008). Another Raman study on the ancient glass artifacts (Ricciardi et al., 2009) showed that the former database of Raman spectra established for enameled glaze were useful to classify the main glass composition types. Characterization of İznik tiles and their copies was carried out by both laboratory type and portable Raman instruments (Simsek et al., 2009). Glazed shards from Macedonia were analyzed by Raman spectroscopy to obtain information on their manufacturing process and provenance (Tanevska et al., 2009). In a recent study, two different types of ancient glasses are examined using the Q_n model and Raman spectroscopy found to be a very useful tool to differentiate glass types (Cesaratto et al., 2010). A number of glass beads from southern Africa were studied by Raman spectroscopy to classify the glass matrix in accordance with previous work and identify the pigments used for coloring (Prinsloo et al., 2011; Tournié et al., 2012).

There are also some remarkable studies which use Raman spectroscopy and X-ray fluorescence spectroscopy for characterization of ancient glasses. As introduced above, Oikonomou et al. (Oikonomou et al., 2008) used Raman spectroscopy for the purpose of evaluation of processing temperatures of fragmented glass beads recovered from Rhodes. Also, a portable XRF spectrometer is used for determination of chemical compositions of the fragments. Chemical compositions were found to be similar to East Mediterranean trends and XRF and Raman Spectroscopy techniques in combination evaluated as valuable non-destructive tools for ancient glass studies. Another study on stained glass fragments belonging to Monastery of Santa Maria da Vito'ria, Batalha, Portugal, was performed by micro XRF and micro Raman analyses. X-ray fluorescence analysis was used to characterize chemical compositions of the glass fragments and corrosion products are analyzed by Raman

spectroscopy. Two major compositional groups have been determined as potash glasses and soda-lime glasses. Calcium carbonate formation as a corrosion product have been shown by Raman spectroscopy (Fernandes, Vilarigues, Alves, & da Silva, 2008). Enameling techniques of Roman glass vessels was the center of attention of a different study carried on by Greiff and Schuster (Greiff & Schuster, 2008). Application of high-lead and soda lime type enamels are determined by micro XRF. Opacifiers such as lead antimonite and calcium antimonite have been determined by Micro-Raman. Another study on ancient Thai glass fragments carried on with both Raman and elemental analyses has revealed that all samples were lead–silica based glasses (Won-in et al., 2011).

Huge collections of glass samples from different archaeological sites remains unanalyzed because reaching the full compositional data is very costly both in manners of time and funds. Raman spectroscopy allowing a comparatively fast classification of different glass types is becoming prominent in the field of characterization of ancient glasses. Nevertheless, comparison of the data derived by Raman spectrometry with another technique giving compositional information is necessary before any conclusions can be drawn. Therefore, the samples were analyzed by Raman spectroscopy first and on the basis of the Raman results, a number of samples are selected for further chemical analysis by XRF in this thesis.

1.3. The Aim and Scope of the Study

The aim of this study is to analyze glass objects that were excavated from Mersin Olba archaeological site by Raman spectrometry and XRF techniques to understand their production techniques, raw materials and period of production. The need for surveying the applicability of Raman spectroscopy on ancient glasses with existing resources and infrastructure in Turkey is also a considerable source of motivation.

Within the frame of this thesis, some glass objects from Mersin Olba archaeological site were attempted to be investigated. The study has been presented in four chapters.

This first chapter includes a brief introduction regarding Raman scattering, descriptions of terms of Q_n model and Polymerization index, a literature review of analysis of ancient glass and glazes by Raman spectroscopy and aim of the study. In the second chapter, definition and general characteristics of glass and ancient glass, history of glass production and description of Olba archaeological site have been shown. Analyzed materials excavated from Olba archaeological site and applied methods in the analysis of those samples have been explained in the third chapter. In the fourth chapter results of the analyses have been discussed in detail. Finally, interpretation of the analytical results has been summarized in chapter five.

CHAPTER 2

THE NATURE OF GLASS AND ITS HISTORY

2.1 The Definition of Glass and Ancient Glass

In a most basic sense, glass is considered as an amorphous material which is a transparent or translucent, brittle solid. . The most common applied method of glass production is cooling of a supercooled liquid (Floudas, Paluch, Grzybowski, & Ngai, 2011). It is possible to cool liquids to develop either a crystal structure or glass structure. If the liquid is cooled to its melting point, liquid phase and the solid phase co-exist and crystallization suddenly takes place. Glass is formed when a liquid is continuously cooled and crystallization is avoided at the same time. A supercooled liquid is acquired if the temperature of the liquid falls below its melting temperature (T_f) without any crystallization. Supercooled liquid turns into a rigid and brittle material. In this context, the formation of glass is a problem of bypassing or avoiding the crystallization (Šesták, Mareš, & Hubík). Production of glass from a liquid is not the only method available. Glass could be formed by methods "such as condensation of vapors on cold substrates, bombardment of crystalline solids by neutrons or by other heavy particles, gelation of solutions followed by removal of solvents, mechanical shear, solvent evaporation or in some cases application of high pressures" (Janssens, 2013; Rao, 2002). American Society for Testing and Materials (ASTM) is defining the glass as 'an inorganic product of fusion which has cooled to a rigid condition without crystallizing'. This definition excludes organic substances such as glycerol and synthetic polymers behaving similar to form glassy state(Šesták et al.) and again does not include all methods of glass production. Even so, above definition is sufficient for explaining ancient and historical glasses (Caddy, 2001; Janssens, 2013; Mark A. Pollard, 2008). With a more comprehensive explanation,

"Glass can be defined as “an amorphous solid completely lacking in long range, periodic atomic structure, and exhibiting a region of glass transformation behavior”. Any material, inorganic, organic, or metallic, formed by any technique, which exhibits glass transformation behavior is a glass" (Shelby, 2005).

Glass can be classified in accordance with their chemical compositions as shown in Table 1. Yet, our scope of interest in this thesis will be limited to ancient glasses which are mainly silicate glasses and especially soda-lime silicate glasses (Mark A. Pollard, 2008).

Table 1. Chemical Classification of Glasses (Janssens, 2013).

	Form of Elements	Chalcogens, metals and alloys
Inorganic	Oxides	Silicates Borates Phospates Vanadates Germanates Tellurites Heavy metal oxides
	Mixed oxides	Oxi-halides Oxi-nitrides Oxcarbides
	Non-oxides	Chalcogenides Halides
Organic	Sugars, glycols, polymers, etc.	

2.2. Silicate Glasses

The term “ancient glasses” is used to refer to silicate glasses produced before the middle of the seventeenth century C.E. (Davison, 2003). Conventional silicate glasses could be defined as “Inorganic non-crystalline products mainly formed by silica which are hard, brittle, generally transparent, having high chemical resistance and deformable at high temperature” (Janssens, 2013). On the other hand, in terms of chemical classification, silicate glasses are a part of oxide glasses which are the

largest group of inorganic glasses. The classical soda-lime glass composition consists of 21.3% Na_2O , 5.2% CaO , and 73.5% SiO_2 (Rasmussen, 2012).

SiO_2 glass structure is composed of SiO_4 tetrahedra units forming a continuous network as shown in Figure 4. Tetrahedra units hold a silicon atom at the center and an oxygen atom at each corner. All four of these oxygen atoms form bridges to silicon atoms of the four neighboring silicon tetrahedra (Davison, 2003).

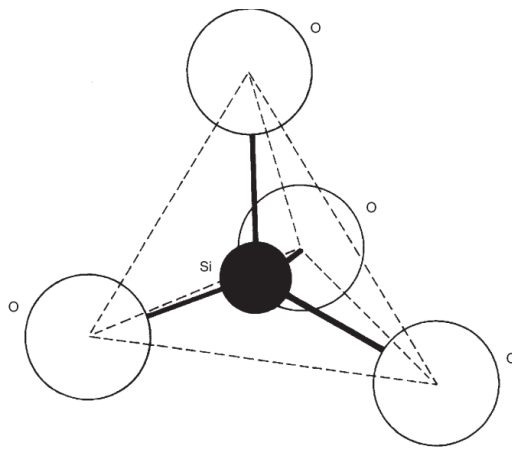


Figure 4. SiO_4 Tetrahedral Unit (Mark A. Pollard, 2008).

SiO_2 glass and SiO_2 crystals are different from each other by the order of SiO_4 tetrahedra network. Tetrahedra units in crystal structure are geometrically and periodically ordered in a regular network, while in the glass such units are randomly distributed, forming a distorted network as shown in Figure 5.

For ancient glassworkers the biggest technical limitation was the requirement of high temperatures to melt raw materials. Since, pure silica glass is not softening until 1500 °C, ancient glassworkers have needed to manipulate the glass structure. Weakening the strong Si-O covalent bonds is the way to decrease the processing temperature. Adding oxides like CaO breaks some of the covalent Si-O bonds and place weaker ionic bonds instead. Weaker bonds mean higher fluidity and thus lower processing temperature of glass.

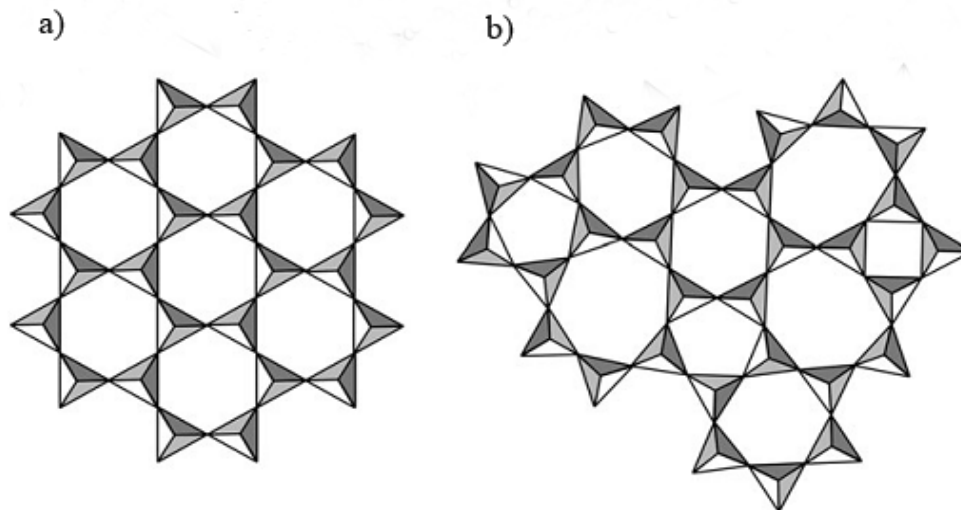


Figure 5. Tetrahedra network structures of a) crystalline vs. b) amorphous SiO₂ phases (Rasmussen, 2012).

If we follow the classification of glass forming oxides as *network formers*, *network modifiers* and *intermediates* (Mark A. Pollard, 2008); we can conclude that SiO₂ is the main *network former* of archaeological glasses.

For changing the chemical and physical properties of the ancient glass by interrupting the continuity of the network, *alkalis* (soda (Na₂O), potash or potassia (K₂O),) and *alkaline earths* (calcia or lime (CaO), magnesia (MgO) and BaO) are used as *network modifiers*. Intermediates improve thermal and mechanical behavior by adding void spaces to the glass structure. Low solubility of these additives increases the resistance of glass to dissolution. Alumina (Al₂O₃) plays an important role in stabilizing the network and PbO is another important of the glassmaking additives used in the production of ancient glasses (Mark A. Pollard, 2008).

2.3. Raw Materials of Ancient Glass

The sand, especially from certain rivers was first to be used as silica source in glass production. Environmental conditions lead to deterioration of rocks and separated small particles accumulates as sand. Therefore, sand from different locations varies

in terms of their compositions. Additives such as calcite (CaCO_3), magnesium oxide (MgO), alumina (Al_2O_3) and iron oxide (Fe_2O_3) were being introduced into the glass structure via sand. These additives affect the stability of the glass. Therefore, search of a purer source of silica has directed ancient glassworkers to use of quartz powder obtained by crushing quartz rocks (Janssens, 2013). Therefore, they used quartz pebbles containing only some trace elements (strontium, barium, cerium) besides silica (Rasmussen, 2012). Belus river was pointed out by Pliny the elder, who has given some early information about the sand sources used as a raw material of ancient glass (Rasmussen, 2012).

Reaching the required heat suitable for melting the silica source down was one of the main difficulties ancient glassmakers had been facing with. As a matter of fact in some cases it was even not possible. It is assumed that the highest temperature ancient glassmakers had reached was not more than $1100\text{ }^\circ\text{C}$ while the melting point of pure silica (quartz) is around $1715\text{ }^\circ\text{C}$. *Soda and Potash* commonly have been used to lower the melting temperature of silica and to make glass mixtures more fusible. Soda was a fluxing agent capable of reducing the melting point less than $1000\text{ }^\circ\text{C}$ and widely used by early glassmakers (Rasmussen, 2012). Furthermore, usage of soda was providing glassworkers a longer amount of time during which glass can be worked on. However, the drawback of soda is making glass susceptible to humidity and carbon dioxide. Presence of water is a principal external force which initiates deterioration of buried glasses. Glasses added to collections after excavated or historical glasses which are not buried are also affected by atmospheric pollution and humidity (Davison, 2003).

Natron, sodium plant ash and potash plant ash were three types of *fluxing agents* (Soda and Potash sources) used in the past (Janssens, 2013). *Natron* is a mixture of evaporate deposits and believed to found in certain regions such as alkali lakes of the Wadi Natrun in Egypt. Sodium bicarbonate, sodium carbonate, sodium sulfate and some organic matter is the main components of natron. It is relatively free of potassium and magnesium, and glasses made with natron usually contain less than

1% MgO and 1% K₂O (Rasmussen, 2012). On the other hand, *sodium plant ash* usually has higher amounts of magnesia and potash than does natron and thus, glasses produced with this flux generally exhibited higher concentrations of potassium oxide (K₂O, 1-4%) and magnesium oxide (MgO, 3-7%) (Rasmussen, 2012).

Melting point lower than 750 °C can be reached by using combinations of soda and calcium as additives, but chemical stability of glass was lowering significantly due to high solubility of sodium (Rasmussen, 2012). Glass is a material that is preferred for being able to colored easily, being transparent as well as its resistance to water and other solvents. Thus, stability of the glass is a quality in demand. As stated before, widespread usage of soda in production was making the early glasses susceptible to humidity and carbon dioxide. Alumina (Al₂O₃) and basic alkaline-earth oxides as CaO and MgO are used as stabilizers to make glass more water resistant (Janssens, 2013). Plant ash and sand containing marine shells were common sources of lime. Magnesium oxide were introduced via ash impurities containing magnesium carbonates or present as the result of corrosion of the clay pot in which the glass is melted (Janssens, 2013). Alumina was probably introduced to the ancient glass as an impurity through non-purified ash and sand. Feldspar and clay particles in sand were the most important source of alumina (Janssens, 2013).

Oxides of transition metals for instance CoO, CuO, FeO, NiO were used in small quantities to color glass objects. Decolorising was another concern of ancient glassmaking. Glass containing iron oxide for example could be decolourised by converting the blue colour of the reduced iron (Fe²⁺) to the yellow colour of the oxidised state (Fe³⁺) by altering the melting conditions or by adding oxidising agents such as the oxides of manganese or antimony to the glass batch. Additionally, antimony was used as an opacifying agent. The source of the antimony was stibnite (Sb₂S₃) used throughout the Mediterranean and the Near East (Rasmussen, 2012).

Table 2. The average composition of some groups of glass found in wrecks (Janssens, 2013).

Origin	II Mill. B.C.	Ulu Burun	Nimrud	Roman	Roman	Early Islamic						
From century	14th B.C.	ca.1300 B.C.	7th B.C.	1st A.D.	1st A.D.	8th A.D.						
To century				4th A.D.	4th A.D.	Early 8th A.D.						
Flux used	Ashes		Transp.	Natron	Natron-ashes	Ashes						
Colour		Blue transp.		Colourless/blue	Pale green	Pale green						
Site found	Amarna Egypt	Ship wreck at Kas Turchia	Mesopotamia	Aquileia	Lattes-Dijon	Raqqa (Syria) –Type 1						
Source	R.H. Brill 1999, II vol. 27	R.H. Brill 1999, II vol. 53	R.H. Brill 1999, II vol. 47	Moretti Gratuze, 2002	Moretti Gratuze, 2002	J. Henderson 1995						
No. samples	9	10	10	10	4	7						
	Ave	Min/Max	Ave	Min/Max	Ave	Min/Max	Ave	+/-				
SiO ₂	64.27	59.61-68.47	67.44	64.24-70.88	66.39	57.97-70.05	68.17	65.8-71.5	63.33	61.8-65.8	67.80	1.20
Al ₂ O ₃	1.70	0.51-3.23	1.76	0.88-2.54	3.01	0.56-7.29	2.69	2.38-3.20	3.09	2.31-4.6	1.10	0.13
MgO	3.98	3.31-4.94	2.88	1.66-4.02	3.33	2.04-4.8	0.51	0.41-0.6	1.72	1.62-1.82	4.50	1.10
CaO	8.30	6.42-9.07	6.87	4.58-8.8	6.82	3.82-10	8.07	7.33-9.37	7.36	6.07-8.55	8.26	1.39
PbO	0.39	0.001-3.72	0.01		1.42	0.001-5.76	0.08	0.001-0.258	0.13	0.07-0.22	0.15	0.05
Na ₂ O	18.38	16.2-20.6	18.45	16.6-20.3	14.82	13-16.5	16.52	14.5-19.5	16.43	14.66-17.4	12.00	0.37
K ₂ O	1.44	0.84-2.53	1.12	0.5-1.6	1.07	0.25-1.54	0.78	0.49-1.10	1.74	1.28-2.19	2.46	0.23
Fe ₂ O ₃	0.63	0.32-0.90	0.63	0.48-0.88	0.80	0.3-1.72	1.03	0.29-1.55	1.62	1.50-1.80	0.44	0.10
TiO ₂	0.10	0.06-0.13	0.09	0.07-0.1	0.13	0.05-0.18	0.05	0.05-0.06	0.20	0.11-0.25	0.10	0.07
Cl					1.14	0.69-1.44	1.07	0.72-1.39			0.72	0.07
SO ₃											0.24	0.07
P ₂ O ₅	0.17	0.01-0.45	0.12	0.02-0.18			0.13	0.09-0.16	0.52	0.18-0.85	0.24	0.10
Sb ₂ O ₃	0.17	0.01-0.45	0.01	0.01	1.47	0.08-3.25	0.42	0.01-3.33	0.04	0.02-0.11		
CuO	0.46	0.015-1.6	0.13	0.05-0.48	0.21	0.005-1.6						
MnO	0.11	0.02-0.19	0.13	0.02-0.33	0.34	0.02-1.55	0.60	0.32-1.01	0.66	0.30-1.02	0.63	0.25

Sb_2O_5 , another source of antimony, as an oxidizing agent, absorbs Fe(II) species to the fairly colorless Fe(III). MnO_2 was used to oxidize the iron and to decolorize the glass. Another important problem during the production of glass is formation of bubbles due to the reaction of soda and lime with silica (Rasmussen, 2012). Manganese oxide was added as a decolorant and also to remove gas bubbles from molten glass.

The average composition of transparent ancient glass types from 6 different sources are listed in Table 2.

2.4. A Brief History of Ancient Glass from the Very First Glass to Roman Glass

2.4.1. Glass from Beginning to the Roman Period

Glass, glaze, enamel and faience and obsidian are vitreous materials which have been a part of material culture of ancient people. Use of the natural glass obsidian by early tribes and even the trade routes of this valuable raw material are well studied by archaeologists. It is acknowledged that usage of vitreous glaze in Mesopotamia, Egypt and Aegean can be dated back to fourth millennium BCE. If we define glass as a transparent, brittle material used to form windows, vessels and many other objects, use of manmade synthetic glass is traced back to 3000 BCE at most (Davison, 2003; Janssens, 2013). With only a few excavated glass discoveries, Mesopotamia (Iraq) is accepted as the birthplace of glass by most of the authorities (Davison, 2003). On the other hand, glass objects dated back to 2500 BCE and 2200 BCE has been excavated in Syria and in Egypt (Rasmussen, 2012).

Starting with Pliny the Elder (AD 23 – August 25, AD 79) some argued that invention of glass could be very likely by chance in Syria, at the mouth of the river Belus. An open fire over the sands at the mouth of river Belus which was accidentally accompanied by natron first caused the invention of glass (Janssens, 2013). Some others believe that production of glass is a byproduct of ancient

metallurgical activities or a logical result of developments in ceramic technology. Presence of copper in a vast number of early glasses is presented as basic evidence that is relating ancient metallurgy to the invention of glass (Rasmussen, 2012).

The first examples were rare, opaque, molded glasses which were probably shaped to imitate semi-precious stones. Polychrome vessels made of mosaic glass followed the use of core-forming technology. Sinking a core (manufactured from clay or some other material) into the molten glass or covering the core with glass by winding glass threads over it were the basis of core forming technology. Development of core-forming technology has opened the way to production of first glass vessels. Few glass items are known until the first core formed vessels were made in western Asia sometime before 1500 BC. Core-forming persisted as an important glassmaking technique for many centuries (Davison, 2003).

Later 15th and 16th centuries BCE was an interval that glassmaking has spread rapidly in Mesopotamia. During this period it is possible to talk about trade of glass as raw material and also as finished objects. In 1500-800 BCE glass production was being performed in certain production sites and ingots and raw materials was carried to some secondary workshops around Mediterranean Region. Glass of this period is described as having typical soda-lime character with high magnesia (3-7%) and potash (1-4%) content, which is representative of glass produced or used throughout the Mediterranean area.

Glassmaking on industrial level in Egypt also began in the 15th century BCE after Egyptian conquests in Syria. After the conquest Syria, glassmaking centers had been emerged in Egypt and succeeded until the 11th century BCE. On site glass production was started in Egypt by 1350 BCE (Rasmussen, 2012). For the period from 1500 BCE to about 800 BCE, it is accepted that quartz pebbles and the ash from halophytic desert plants were main ingredients of glass in both the Near East and Egypt (Rasmussen, 2012).

The period between the end of the 2nd and beginning of the 1st millennium BCE is considered to be a lost era regarding the glassmaking based upon the absence of glass finds from this period (Davison, 2003). That phase has been overwhelmed by rebirth of great empires and 9th century BCE is indicated as the time of revival of glass industry. Between 550 to 50 BCE core formed glass objects have become widespread (Davison, 2003).

Antimony-rich glass is very extensive during the period of 6th century BCE to about 4th century CE (Rasmussen, 2012). Along with its antimony rich nature, low potassium (0.1-1.0%) and magnesium (0.5-1.5%) content is another characteristic of the glass of this period (Rasmussen, 2012).

Transparent and closer to colorless mold-cast glass was the characteristic during the Hellenistic Period (late 4th to 2nd century BC) (Davison, 2003). Alexandria founded by Alexander the Great in 332 BCE was the main glassmaking center of Hellenistic civilization. Soda glass allowing the production of larger objects was common in Hellenistic period. Natron and sand use as raw materials were sustained. Generally the alumina content of these glasses is approximately 2.5% by weight, potassium and magnesium oxides are both less than 2% and calcium oxide is between 6–9%. In sodic glass, the proportion of sodium oxide (Na₂O) and silica (SiO₂) vary somewhat from one sample to another, usually within the range of 14% to 18% and 60% to 70%. This composition was used to form blown glass in the late first century B.C.E. to the early first century C.E. and then it was preferred for the next 700 years or so. It is now considered that early raw glass was produced in the Near East and shipped to various glassworking sites to finalize production in this era (Janssens, 2013).

2.4.2. Roman Glass

Sand was typically used as the silica source in Roman period, rather than the ground quartz pebbles choice of the previous periods of glass production. The increased alumina content of the Roman glass is considered to be an indicator to prove the use

of sand as the silica source (Mark A. Pollard, 2008; Rasmussen, 2012). In company with the change in the silica source, choice of the decolorant is another significant feature of Roman glass which differentiates it from previous antimony-rich glasses. The change from *antimony to manganese* as the decolorant is the major change used as raw materials for Roman glass production. The production of transparent glasses containing manganese dates back to the 1st century BCE (Rasmussen, 2012). Regarding chemical content the Roman glass is generally uniform. This uniformity implies the existence of common production centers (Rasmussen, 2012). Although, the actual locations of Roman glassmaking sites are unknown, very limited production sites assumed to exist in the Near East where there is a good source of natron and sand (Mark A. Pollard, 2008).

Roman Period and especially 1st to 4th century CE generally considered as *Golden Age of Glass*. In this period, glass production and usage became widespread (Janssens, 2013; Rasmussen, 2012). In the 1st century, window glass was first become available and household use of specific kinds of glass was become common in the 3rd century (Rasmussen, 2012). Glassblowing technology has caused the revolutionary change in glassmaking. Glass has been turned into a cheap commodity which could be mass produced throughout the Roman Empire (Janssens, 2013).

Glass vessels of the Byzantine period (4th to 7th centuries CE) demonstrate imagination and great technical skill, but the forms are rather heavy (Davison, 2003). Being similar to Roman glass composition, Byzantine production shows signs of the change in glass composition due to the change in the use of soda source. After the total disintegration of Roman system which had been made accessing mineral soda sources possible for an extensive geography, soda was again extracted from halophytic plant ashes (Janssens, 2013).

A change in the glass composition begins to occur in the 9th and 10th centuries CE. This composition shift has been noted to reflect the use of plant ash from halophytic plants instead of mineral natron sources (Janssens, 2013). It is known that

transformation from *mineral to plant ash soda* was a consequence of the loss of natron sources in Egypt.

2.5 Olba Archaeological Site

Olba Region is located between the rivers Göksu in Silifke and Lamas (Lamos) in Erdemli. It is one of the best documented regions of Rough Cilicia (Durukan, 2005) (Figure 6). Olba consists of an antique acropolis settled on a hill and necropolis areas surrounding the acropolis. In the Hellenistic and Roman periods, it was a city mainly relying on agriculture and associated with Diocaesarea a religious and administrative center of this region.

Religious structures, aqueducts, necropolis, nymphaeum, theatre, towers, cistern are some remains existing in Olba Archaeological site. Inside the acropolis is a poorly preserved building, possibly a temple, with elements of Corinthian order datable to the 2nd century AD. Tombs, houses and cisterns are also inside the acropolis walls. Outside the walls are a theatre, a nymphaeum, an aqueduct and traces of the walls of a bathhouse. On the north and south slopes of the acropolis were residential areas, but no domestic installations were found in the Doğu Vadisi (East Gorge), where there are remains of what may be churches and a monastery. Remains of residential buildings and tombs of various types is the evidence for a relatively high population. The archaeological surveys in Olba, initiated in 2001 with the permission of the Ministry of Culture and Tourism and the financial support of the Rectorate of Mersin University. Surveys have been conducted at the site since 2001 by Prof. Dr. Emel Erten of Mersin University (Erten, 2007).

Glass finds made available by Olba archaeological excavations since 2010 shows that glass was an ordinary part of material culture. Furthermore some slag samples among these finds shows the possibility of local glass working at the site (Erten, 2003). The glass finds from Olba came from the rock-cut cultic grounds, the Monastery, church, acropolis and Şeytan Deresi Valley. The excavated samples

include the fragments of Late Hellenistic and Roman vessels, late antique goblets and lamps and windows panes.

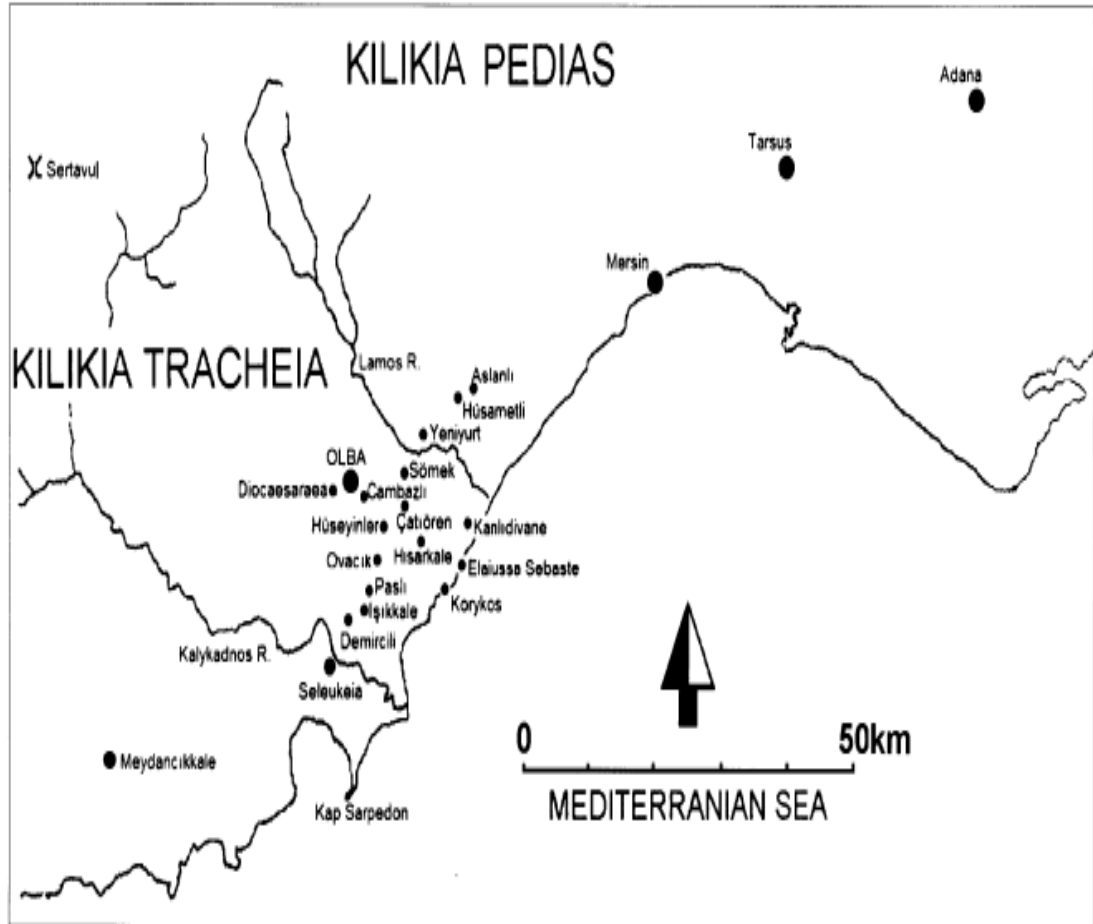


Figure 6. Cilicia and Olba region (Durukan, 2005).

CHAPTER 3

MATERIALS AND METHODS

In this study, 34 glass samples recovered in the excavations at Mersin Olba archaeological region was characterized by Raman spectroscopy and PED-XRF to get information about the raw materials and production technology of ancient Olba glasses.

3.1. Glass Samples Excavated from Olba Archaeological Site

34 window glass fragments excavated from different depths and areas of the Olba archaeological site were photographed and characterized by Raman and XRF spectroscopy. The microscopic images during the Raman analysis samples were also taken under the optical microscope attached to the Raman spectrometer. Information regarding the archaeological context of the glass pieces is given in Table 3. The optical images of the samples are presented in Appendix A and the thicknesses of the glasses determined by vernier caliper are listed in Appendix B.

Table 3. Information on archaeological context of Olba glass samples.

Sample	Excavation Area	Excavation Date	*Depth (cm)
2a	Theatre	13.07.2011	44
3a	Theatre	14.07.2011	36
4a	Theatre	14.07.2011	65
5a	Theatre	15.07.2011	42-85 North/10-120 South
6a	Theatre	16.07.2011	120

Table 3. (continued)

Sample	Excavation Area	Excavation Date	*Depth (cm)
7a	Theatre	18.07.2011	160
12a	Theatre	22.07.2011	134
14a	Theatre	23.07.2011	155
15b	Theatre	25.07.2011	120
16a	Theatre	26.07.2011	157
16b	Theatre	26.07.2011	157
19b	Theatre	27.07.2011	205
28	Theatre	05.08.2011	260
29	Theatre	06.08.2011	100
32	Theatre	14.07.2012	65-81
33	Theatre	17.07.2012	143-184
38a	Theatre	19.07.2012	95-115
39	Theatre	17.07.2012	50
43b	Theatre	25.07.2012	20-40
46	Theatre	24.07.2012	20-40
52	Theatre	04.08.2012	110
57a	Theatre SE South	2010	207
59b	Theatre SE North	12.08.2010	
61a	Theatre SE South	13.08.2010	222
63c	Theatre SE	16.08.2010	
65a	Theatre SE South	10.08.2010	
70a	Theatre SE North	09.08.2010	120
74a	Acropolis South	19.08.2010	
78	Church	21.07.2011	60
79	Church	22.07.2011	100-115
80b	Church	23.07.2011	79-100
84b	Church	01.08.2011	43-120
87b	Monastery	01.08.2012	

*Measured from the surface

3.2. Raman Spectroscopic Analysis of the Samples

The Raman spectroscopic analyses of the 34 glass samples were recorded on a Bruker Senterra micro Raman spectrometer in the Materials Conservation Laboratory (MCL) of the Department of Architecture, Middle East Technical University. The spectrometer is equipped with a diode laser operated at 100 mW with a wavelength of 785.0 nm. The spectra were taken with a resolution of $\sim 9 \text{ cm}^{-1}$. The Raman spectra were collected by manually placing the 50x lens near the desired point of the sample on silicon wafer and all the spectra were calibrated according to the silicon peak at 522 cm^{-1} .

Method of analysis of Raman spectrum data derived from glass samples has been settled through the last decade (Cesaratto et al., 2010; Ph Colomban & Treppoz, 2001; Philippe Colomban, 2003b, 2008; Philippe Colomban, Etcheverry, et al., 2006; Philippe Colomban et al., 2004; Philippe Colomban, Tournie, et al., 2006; Ricci et al., 2007; Robinet et al., 2006; Simsek et al., 2009; Tanevska et al., 2009). A boson peak and two broad bands are three main components of the Raman spectra of silicate glasses. Although the origin of the Boson peak is much debated, it is a general characteristic of the glassy state appears in the Raman spectrum. One of the arguments about the formation of the Boson peak is due to the soft potential model derived from the two-level model of localized oscillators in an-harmonic double potential wells (McIntosh, Toulouse, & Tick, 1997). The other one is that the peak is formed due to scattering from acoustic propagating in a disordered medium (McIntosh et al., 1997). Eliminating the Boson peak and retaining only Si-O bending and stretching modes are the main objectives of the baseline subtraction. All collected Raman spectra of glass samples were baseline corrected using Origin 8.5 software in this study. The junction points were minimized to 4 in most cases to isolate only two strong Si-O bands and to attach the baseline for each spectrum at about the same wavenumber and not lose the originality of the spectrum. Four segmented linear baseline is subtracted at around 150, 720, 850 and 1300 cm^{-1} .

Deconvolution of the Raman spectrum components was carried out using Originpro software using Q_n method^{13f, 13g} explained in detail in Section 1.2.1. The literature data (Philippe Colomban, 2003b; Philippe Colomban & Paulsen, 2005), regarding the assigned wavenumbers for the 5 Q components are given in Table 4.

Table 4. Literature data, regarding the assigned wavenumbers for 5 components.

Assignment	Component	Wavenumber (cm⁻¹)
Zero bridging oxygens	(Q ₀ or monomer, i.e. isolated SiO ₄)	800–850
One bridging oxygens	(Q ₁ or Si ₂ O ₇ groups)	950
Two bridging oxygens	(Q ₂ or silicate chains)	1050–1100
Three bridging oxygens	(Q ₃ or sheet-like region)	1100
Four bridging oxygens	(Q ₄ , SiO ₂ and tectosilicates)	1150–1250

For a number of glass objects (15b, 80b, 84b, 14a, 28, 32, 43b, 5a), Q₃ and Q₄ components are assigned as one peak (Philippe Colomban & Paulsen, 2005), since the differentiation between these components are sometimes difficult due to the low intensity of Q₄ component (Philippe Colomban & Tournié, 2007). In some of the glass samples, one or two narrow bands are added in order to take crystalline phase into account in line with the literature data (Philippe Colomban, 2003b; Philippe Colomban & Paulsen, 2005). A Gaussian shape is assumed for all Raman peaks in this study.

Similarly, 5 components (considering Q₀ as a part of bending mode too) were assigned for bending band of the spectrum too. Low wave number peaks, <300 cm⁻¹, are added to represent the boson contribution (Philippe Colomban & Paulsen, 2005). After deconvolution process, the integral area, the bandwidth and the center of

gravity for each component was calculated. Though extra peaks is not belong to the signature of the glassy silicate network, they are not included in the calculation of Polymerization index (Philippe Colomban, 2008).

3.3. X-Ray Fluorescence (XRF) Analysis of Glass Samples

Polarized energy dispersive X-Ray Fluorescence spectrometer (PED-XRF) was used for the elemental analysis of the Olba glass samples. The samples were analyzed using the SPECTRO XLAB 2000 Model PED-XRF instrument at Earth Sciences Application and Research Center (YEBİM) of Ankara University. The instrument is equipped with a 400W Rh anode X-ray tube and has a liquid nitrogen-cooled Si(Li) detector. The resolution values were <150 eV Mn K α , 5000 cps.

The glass samples were first grinded into a fine powder using an agate mortar and pestle for XRF analysis. The samples were sieved to pass through 200 μ m filter and then, pressed into thick pellets of 32 mm diameter using wax as binder and finally XRF analysis of these pellets was performed.

A certain portion of every sample (0.3 g) were first dried at ashed at 105°C for 6 hours and then, ashed at 950°C for 1 hour in order to calculate loss on ignition (LOI). LOI is calculated in accordance with the formula below:

$$\text{L.O.I. (weight \%)} = ((n_2 - n_3) / (n_2 - n_1)) * 100$$

where, n_1 : weight of the empty crucible, n_2 : weight of the empty crucible plus sample powder, n_2 : weight of the empty crucible plus sample powder, n_3 : weight of the empty crucible plus sample powder after ignition.

CHAPTER 4

RESULTS AND DISCUSSION

4.1. XRF Analysis of the Olba Glass Samples

Major, minor and trace elements of 34 glass samples were determined using XRF technique. Chemical composition of the glass samples is given in Table 5, Table 6, Table 7 and Appendix A, B, C, D. Values are given as percentage (g of element or oxide per hundred grams of glass sample) or ppm (as mg of element or oxide per kg of glass samples). XRF results of 34 glass samples from Olba archaeological site shows that the main network former of the Olba glass samples is silica, main fluxing agent is soda and main stabilizer is lime. Silica concentration of the glass samples varies between 42% and 65% by weight with the average value of $55\pm 5\%$. In glass samples, concentration of oxides are: Na_2O (soda) as fluxing agent between 4.8% and 12.7% ($8.9\pm 1.9\%$); CaO as stabilizer between 5.7% and 9.9% ($7.2\pm 0.9\%$); K_2O (potash) as fluxing agent between 0.55% and 0.94% ($0.72\pm 0.08\%$); MgO as stabilizer content between 0.2% and 0.6% ($0.4\pm 0.1\%$); Al_2O_3 between 0.6 % to 1.4 % ($0.9\pm 0.2\%$).

Silica is responsible for the structure of glass. The source in glass samples is either sand (especially from rivers) or quartz rocks (Davison, 2003; Janssens, 2013). CaCO_3 , MgO , Fe_2O_3 and Al_2O_3 are well-known impurities introduced into the glass by sand¹. If sand is crushed, grinded or washed before, a decrease in the concentration of these impurities and a relative increase in silica concentration is observed (Dieter Brems et al., 2012).

Table 5. Percent composition of the Olba glass samples.

Sample Code	Na ₂ O	MgO	Al ₂ O ₃	SiO ₂	P ₂ O ₅	SO ₃	Cl
12a	11.69	0.49	1.30	63.9	0.077	0.055	0.79
14a	7.19	0.30	0.90	55.7	0.003	0.082	0.62
15b	6.20	0.28	0.71	52.4	0.003	0.131	0.52
16a	10.55	0.44	1.23	60.6	0.076	0.133	0.67
16b	7.23	0.26	0.72	47.3	0.003	0.048	0.65
19b	6.82	0.41	0.81	54.8	0.003	0.080	0.57
28	4.77	0.25	0.70	48.2	0.003	0.087	0.50
29	8.17	0.38	0.78	49.6	0.02	0.102	0.56
2a	8.79	0.40	0.99	59.0	0.043	0.129	0.67
32	9.64	0.52	1.07	56.2	0.055	0.058	0.63
33	8.18	0.31	0.92	53.9	0.003	0.001	0.68
38a	12.69	0.50	0.58	55.0	0.018	0.253	0.76
39	6.32	0.29	0.75	42.0	0.051	0.044	0.49
3a	10.09	0.46	0.93	56.8	0.003	0.128	0.78
43b	10.11	0.42	0.64	50.7	0.02	0.186	0.61
46	9.20	0.41	0.98	56.4	0.045	0.069	0.65
4a	8.39	0.50	0.95	55.8	0.012	0.125	0.64
52	11.18	0.50	1.14	61.8	0.077	0.102	0.74
57a	7.36	0.39	0.80	58.1	0.003	0.190	0.56
59b	8.67	0.37	0.96	59.2	0.003	0.220	0.72
5a	9.89	0.51	1.05	48.5	0.003	0.194	0.55
61a	10.00	0.52	1.33	64.7	0.063	0.017	0.82
61b	7.94	0.41	0.99	58.7	0.003	0.120	0.63
63c	10.70	0.55	1.30	59.8	0.064	0.045	0.73
65a	10.55	0.60	1.42	60.4	0.058	0.047	0.74
6a	6.61	0.30	0.87	45.1	0.003	0.039	0.54
70a	5.93	0.16	0.58	49.1	0.003	0.040	0.63
74a	6.11	0.27	0.82	49.0	0.007	0.001	0.48
78	10.80	0.41	1.02	60.6	0.013	0.083	0.84
79	11.98	0.57	0.69	51.9	0.017	0.268	0.65
7a	8.86	0.45	1.04	55.5	0.022	0.037	0.63
80b	10.31	0.43	0.91	57.5	0.036	0.134	0.72
84b	9.95	0.53	0.98	56.9	0.061	0.091	0.60
87b	9.38	0.48	1.13	57.7	0.003	0.089	0.73

Table 6. Percent composition of the Olba glass samples and LOI values.

Sample Code	K ₂ O	CaO	TiO ₂	V ₂ O ₅	Cr ₂ O ₃	MnO	Fe ₂ O ₃	*LOI
12a	0.73	7.87	0.10	0.003	0.006	0.07	0.58	12.6
14a	0.67	6.69	0.08	0.001	0.004	0.06	0.57	27.7
15b	0.72	6.81	0.09	0.001	0.004	0.24	0.68	31.9
16a	0.89	8.47	0.11	0.004	0.003	0.06	0.59	16.8
16b	0.64	6.04	0.06	0.004	0.002	0.02	0.32	37.0
19b	0.59	6.53	0.09	0.004	0.003	0.11	0.60	28.9
28	0.65	6.38	0.08	0.001	0.004	0.08	0.62	37.6
29	0.73	6.77	0.09	0.004	0.003	0.30	0.61	31.4
2a	0.74	7.36	0.10	0.003	0.003	0.18	0.62	20.6
32	0.74	9.92	0.11	0.005	0.011	0.14	0.67	20.4
33	0.74	6.80	0.08	0.004	0.002	0.02	0.47	27.8
38a	0.64	6.17	0.13	0.004	0.002	0.80	0.78	21.6
39	0.64	7.01	0.09	0.004	0.004	0.15	0.60	41.8
3a	0.67	7.18	0.08	0.002	0.004	0.02	0.41	22.5
43b	0.70	6.44	0.12	0.004	0.004	0.61	0.66	28.6
46	0.76	7.48	0.10	0.004	0.003	0.21	0.66	23.9
4a	0.70	7.19	0.09	0.004	0.004	0.17	0.62	23.1
52	0.79	7.94	0.11	0.002	0.005	0.21	0.64	15.0
57a	0.75	6.21	0.08	0.001	0.004	0.02	0.39	25.0
59b	0.70	6.06	0.08	0.003	0.004	0.02	0.37	22.8
5a	0.55	5.72	0.12	0.005	0.004	1.07	0.83	30.8
61a	0.75	8.10	0.10	0.004	0.003	0.03	0.47	13.5
61b	0.74	8.16	0.10	0.005	0.004	0.08	0.70	21.7
63c	0.71	8.59	0.12	0.003	0.006	0.08	0.68	16.6
65a	0.72	8.51	0.14	0.005	0.009	0.08	0.68	16.9
6a	0.67	6.62	0.09	0.005	0.002	0.13	0.58	39.0
70a	0.78	5.98	0.05	0.001	0.004	0.01	0.28	36.0
74a	0.94	7.67	0.07	0.001	0.002	0.08	0.34	34.9
78	0.88	7.20	0.09	0.002	0.002	0.04	0.40	17.5
79	0.65	6.30	0.13	0.004	0.002	0.53	0.72	25.9
7a	0.72	7.97	0.10	0.002	0.005	0.12	0.64	23.6
80b	0.68	7.40	0.09	0.002	0.005	0.78	0.49	20.5
84b	0.78	8.40	0.12	0.006	0.005	0.23	0.71	20.6
87b	0.69	8.23	0.10	0.004	0.004	0.06	0.66	20.6

* Loss on ignition at 950 C⁰

Table 7. Average percent composition of the Olba glass samples.

	Average	Standart Deviation
Na ₂ O	8.9	1.9
MgO	0.4	0.1
MnO	0.2	0.2
Al ₂ O ₃	0.9	0.2
SiO ₂	55	5
P ₂ O ₅	0.03	0.03
Cr ₂ O ₃	0.004	0.002
SO ₃	0.1	0.07
Fe ₂ O ₃	0.6	0.1
Cl	0.6	0.1
CaO	7.2	1.0
K ₂ O	0.72	0.08
TiO ₂	0.1	0.02
V ₂ O ₅	0.03	0.01
*LOI	25.1	7.7

“A positive correlation between iron and phosphorus, alumina and titanium suggests that these oxides originates from the same glass-forming raw materials” (Jackson, 2005). A strong correlation between Fe₂O₃ concentration and TiO₂ concentration is shown in Figure 7. Two positively correlated groups are identified from Figure 7. First group consists of the samples with Fe₂O₃ concentration below 0.5% shown as light blue dots and the second group containing higher than 0.5% Fe₂O₃ concentration shown as dark blue dots. Furthermore, rate of increase of 2nd group is higher with respect to the 1st group.

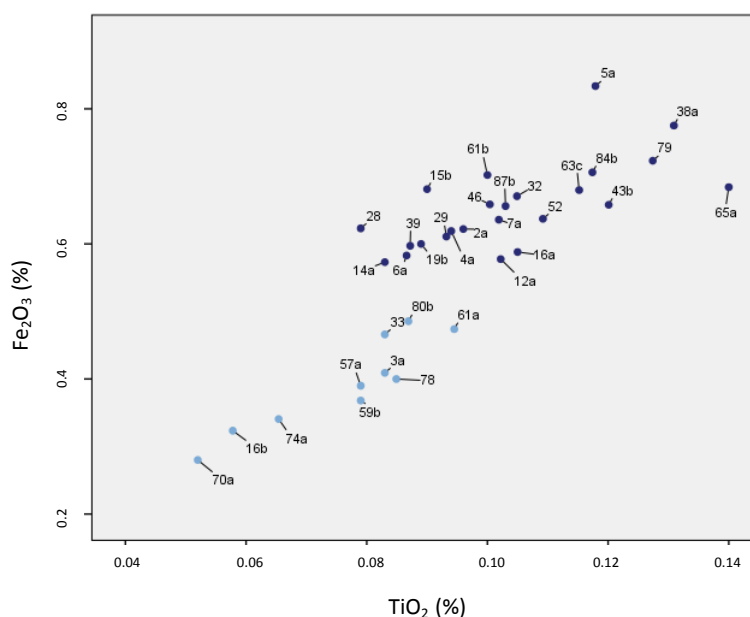


Figure 7. The scatter plot of TiO₂ concentration vs. Fe₂O₃ concentration of 34 Olba glass samples.

As seen in Figure 8, a direct correlation between Fe_2O_3 and SiO_2 concentration does not exist. On the other hand, for samples 16b, 74a, 70a, 33, 80b, 3a, 57a, 59b, 78 and 61a which have iron less than 0.5%, Fe_2O_3 concentration is positively correlated with SiO_2 content. Therefore, it is possible that there could be two different source of Fe_2O_3 in Olba glass samples. Fe_2O_3 may be introduced to the samples 16b, 74a, 70a, 33, 80b, 3a, 57a, 59b, 78 and 61a form silica source as an impurity and for the rest of the samples, the source may be due contamination through glassmaking process and/or addition of an ingredient which is the source of both TiO_2 and Fe_2O_3 since they show a positive correlation as shown in Figure 7.

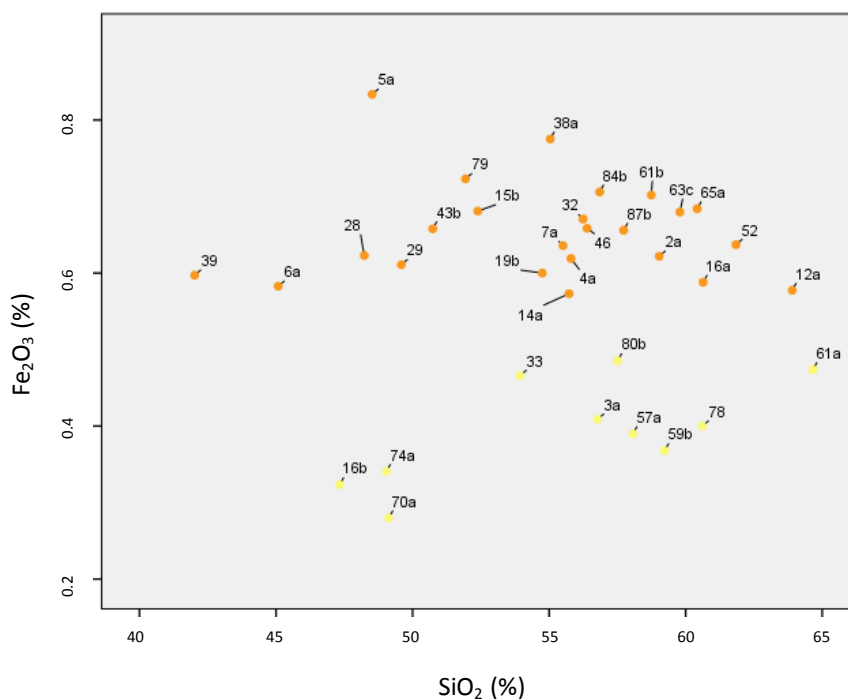


Figure 8. The scatter plot of SiO_2 concentration vs. Fe_2O_3 concentration of 34 Olba glass samples.

Figure 9 shows a similar trend with respect to two groups suggested by the correlations among TiO_2 , Fe_2O_3 and SiO_2 . Samples 16b, 74a, 70a, 33, 80b, 3a, 57a, 59b, 78 and 61a, Fe_2O_3 values are positively correlated with Al_2O_3 values.. For the rest of the samples there is no correlation found between Fe_2O_3 and Al_2O_3 concentration. In Figure 9 samples represented by light green dots form a group similar to that observed in Figure 7 and Figure 8.

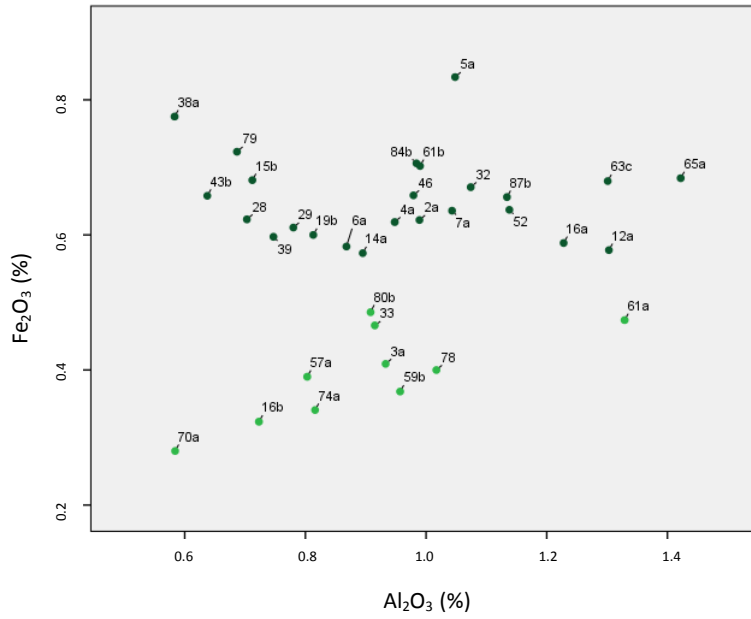


Figure 9. The scatter plot of Al₂O₃ concentration vs. Fe₂O₃ concentration of 34 Olba glass samples.

The scatter plot between SiO₂ and Al₂O₃ results is given in Figure 10. Positive correlation between concentration of SiO₂ and Al₂O₃ may indicate that Al₂O₃ is also introduced into the Olba glass together with the silica source.

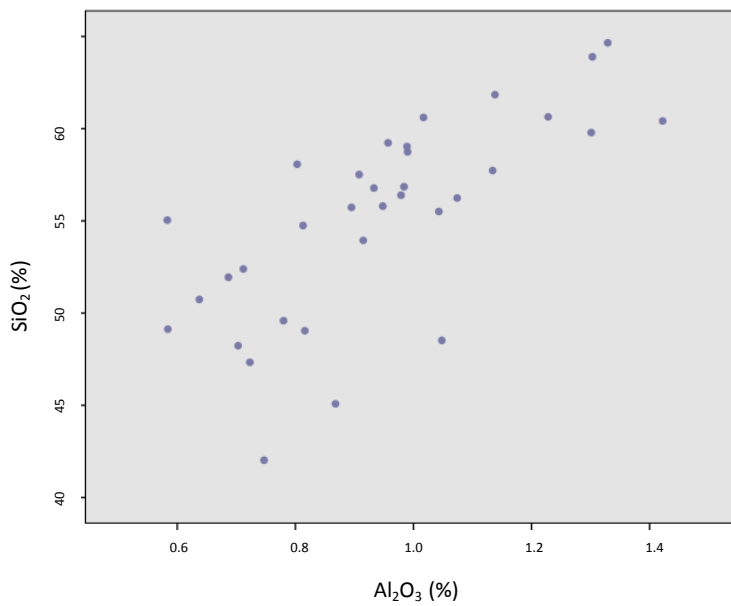


Figure 10. The scatter plot of Al₂O₃ concentration versus SiO₂ concentration of 34 Olba glass samples.

Al_2O_3 is acknowledged as a universal component of historical/ancient glasses. Al_2O_3 concentration in ancient glasses generally varies in the range of 1-5% by weight (Beşer, 2009). The average Al_2O_3 concentration of Roman glasses is around 2.7% as seen in Table 2 however, the alumina contents of natron are reported very lower, typically less than 0.5% (R.H. Brill, 1999). This is probably due the use of pure sand as silica source (Shortland, Schachner, Freestone, & Tite, 2006).

There is a strong positive correlation between CaO and SiO_2 concentration of Olba glass samples. That means, CaO was not added to batch deliberately and the silica source is probably sand. If natron is the source of fluxing agent for Olba glass samples, average Al_2O_3 content of $1\% \pm 0.2$ may suggest that relatively pure sand was used as silica source.

Al_2O_3 and CaO levels of glass samples are positively correlated as shown in Figure 11. This strong correlation suggests that CaO and Al_2O_3 are originated from same source and this source most probably is sand since both CaO and Al_2O_3 are positively correlated with SiO_2 . It is known that CaO added with sand is generally originating from shell fragments or eroded limestone (Davison, 2003).

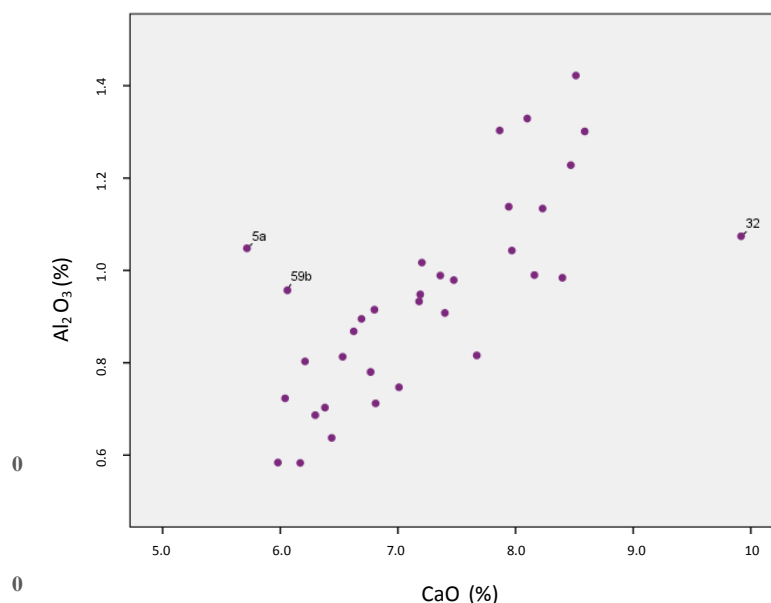


Figure 11. The scatter plot of Al_2O_3 concentration versus CaO concentration of 34 Olba glass samples.

High level of strontium (c. 400 ppm) and low level of zirconium (c. 60 ppm) is considered as an indicator of the use of coastal sand for glass production (Freestone, Leslie, & Thirlwall, 2003; Henderson, 2013). Strontium level of the Olba glass sample is ranging from 407 to 564 ppm (493 ± 39 ppm). For Olba glasses, zirconium concentration is between 39 to 90 ppm. Therefore, mature coastal sand might be used as silica source in production of Olba glass samples.

Olba glass samples contain Na_2O as the principal fluxing agent with an average concentration of $8.9\pm 1.9\%$. Typical ancient soda-lime-silica glasses are estimated to have a concentration of Na_2O above 14% (Janssens, 2013). In point of fact soda content should be higher if cast glass aimed to be produced. Lower soda concentration of Olba glass samples suggests that higher temperatures were used during the production process. Low Na_2O content is also related to recycling of glass objects (Towle, 2002). Concentrations of Mn, Co, Ni, Cu, Zn, As, Se, Ag, Cd, In, Sn, Sb, and Pb between 100 and 1000 ppm are typically interpreted as an indication for glass recycling (D. Brems & Degryse, 2014). Nevertheless this is not the case for Olba glasses since the concentration of only Pb is high enough to relate low Na_2O with recycling of Olba glass objects.

The concentration of K_2O and MgO in typical natron glasses is reported as less than 1% and the concentration P_2O_5 is reported as about 0.1-0.2% in a 10% soda glass (R.H. Brill, 1999). The potash and magnesia concentration of all Olba glass samples are both less than 1% and P_2O_5 content is lower than 0.1%. Therefore, it is highly probable that soda source of Olba glasses is natron.

Manganese is introduced into the glass by sand, by flux or intentionally (Towle, 2002). Manganese is not present in natron, and only appears in glassmaking sand at low levels (lower than 0.1% in general and up to 0.5% in sands from the River Volturno) (R.H. Brill, 1999; Jackson, 2005). Therefore, its presence in a natron-type soda lime silica glass above 0.1% indicates its deliberate addition (Towle, 2002). MnO concentration in Olba glasses is ranging between 0.01 to 1% ($0.2\pm 0.2\%$).

Interestingly, as seen in Figure 12, for samples with Fe_2O_3 lower than 0.5%, MnO levels are very low (around 0.02%) MnO concentration of glass samples 16b, 74a, 70a, 33, 3a, 57a, 59b, 78 and 61a is close to each other around 0.07% MnO. For the rest of the samples, a strong positive correlation is observed between Fe_2O_3 and MnO concentration as shown in Figure 13. From this strong correlation between MnO and Fe_2O_3 results, we can conclude that their sources are same for these glass samples since MnO concentration range in Olba glass samples indicates its deliberate addition. Fe_2O_3 for samples 12a, 14a, 15b, 16a, 19b, 28, 29, 2a, 32, 38a, 39, 43b, 46, 4a, 52, 5a, 61b, 63c, 65a, 6a, 79, 7a, 80b, 84b and 87b may be originated from the ingredient which was used to add MnO intentionally.

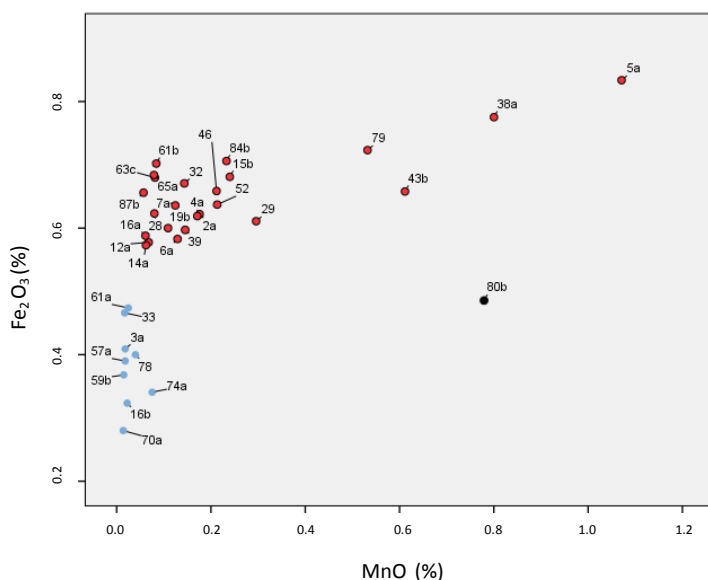


Figure 12. The scatter plot of Fe_2O_3 concentration vs. MnO concentration of 34 Olba glass samples.

4.2. Raman Spectroscopic Analysis of Olba Glass Samples

In line with the procedure explained in Chapter 3, background is subtracted from Raman spectra of all of the Olba glass samples. Representative raw and baseline corrected spectra for the Mersin Olba glasses are given in Figure 13, Figure 14, Figure 15 and Figure 16. As shown in Figure 15, the background of Raman spectra is very high and this is resulted in low signal to noise ratio. As a result of their high

background signal, it is not possible to discriminate the Q_0 peak expected between 700 and 800 cm^{-1} wavenumbers. I_p index values of these samples are also calculated higher compared to the others. On the other hand, S/N ratio of Raman spectra of the samples represented in Figure 15 and Figure 16 are high enough to locate the position of Q_0 peak.

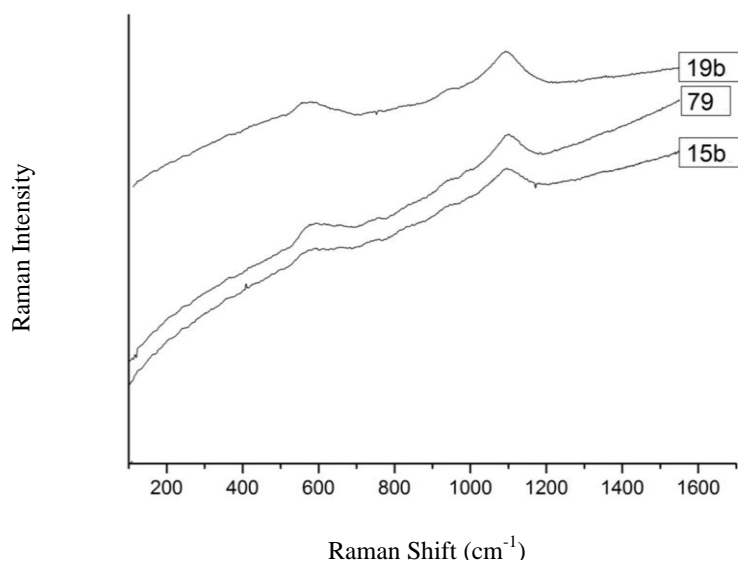


Figure 13. Raw Raman spectra of glass samples, 19ba, 79a, and 15ba.

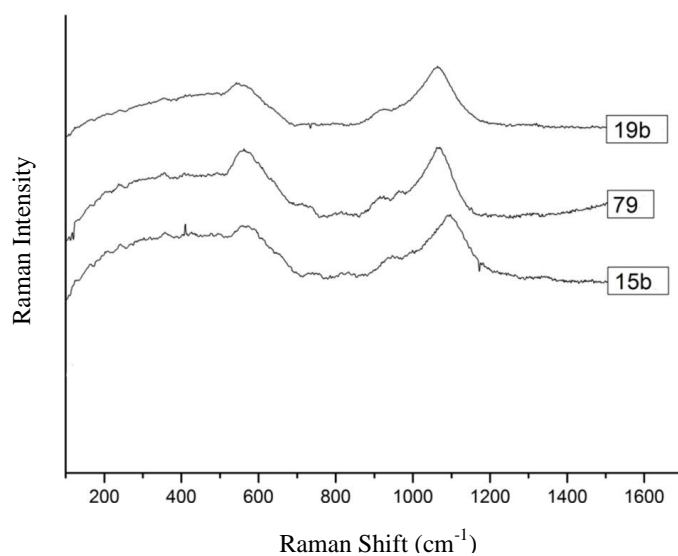


Figure 14. Baseline corrected Raman spectra of glass samples, 19ba, 79a, and 15ba.

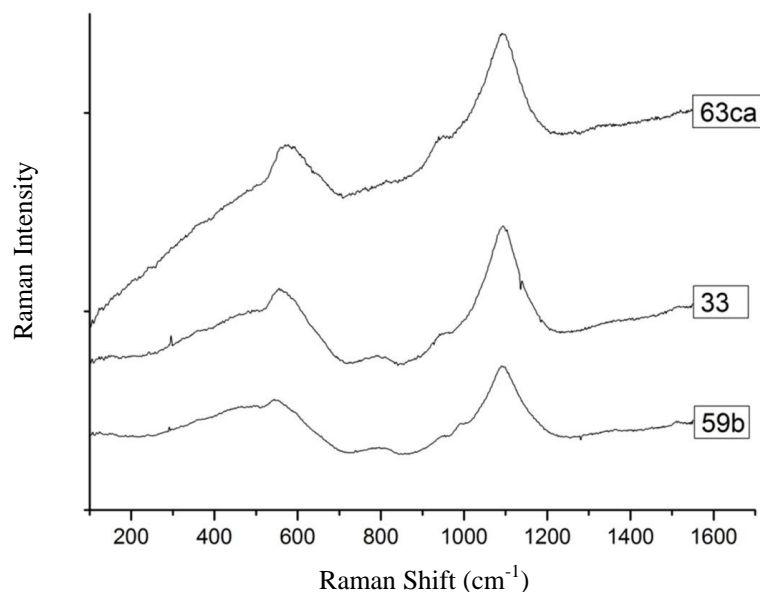


Figure 15. Raw Raman spectra of glass samples, 63ca, 33b, 59b.

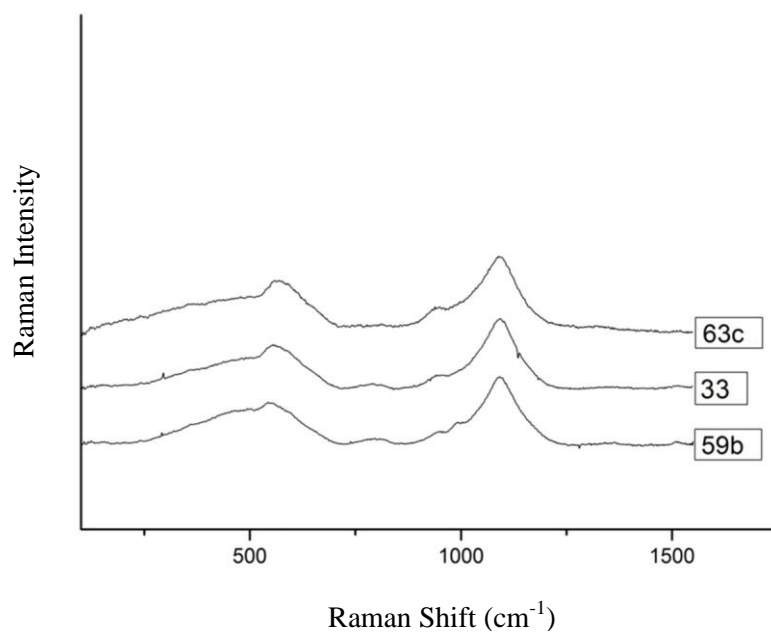


Figure 16. Baseline corrected Raman spectra of glass samples, 63ca, 33b, 59b.

Deconvoluted spectra of glass samples 15b, 19b, 79, 33, 59b, and 63c are shown in Figure 17. As can be seen in the Figure 17, bending modes of samples 15b, 19b and 79 are broader compared to those shown in samples 33, 59b and 63c. This broadening in bending mode resulted in relatively large deviations in I_p values.

As explained in section 1.2.1, I_p index values are calculated using the intensities of Si-O bending and Si-O stretching modes. It was very difficult to deconvolute Q peaks under Si-O bending peaks if the signal to noise ratio is low and/or bending mode in Raman spectra is broad.

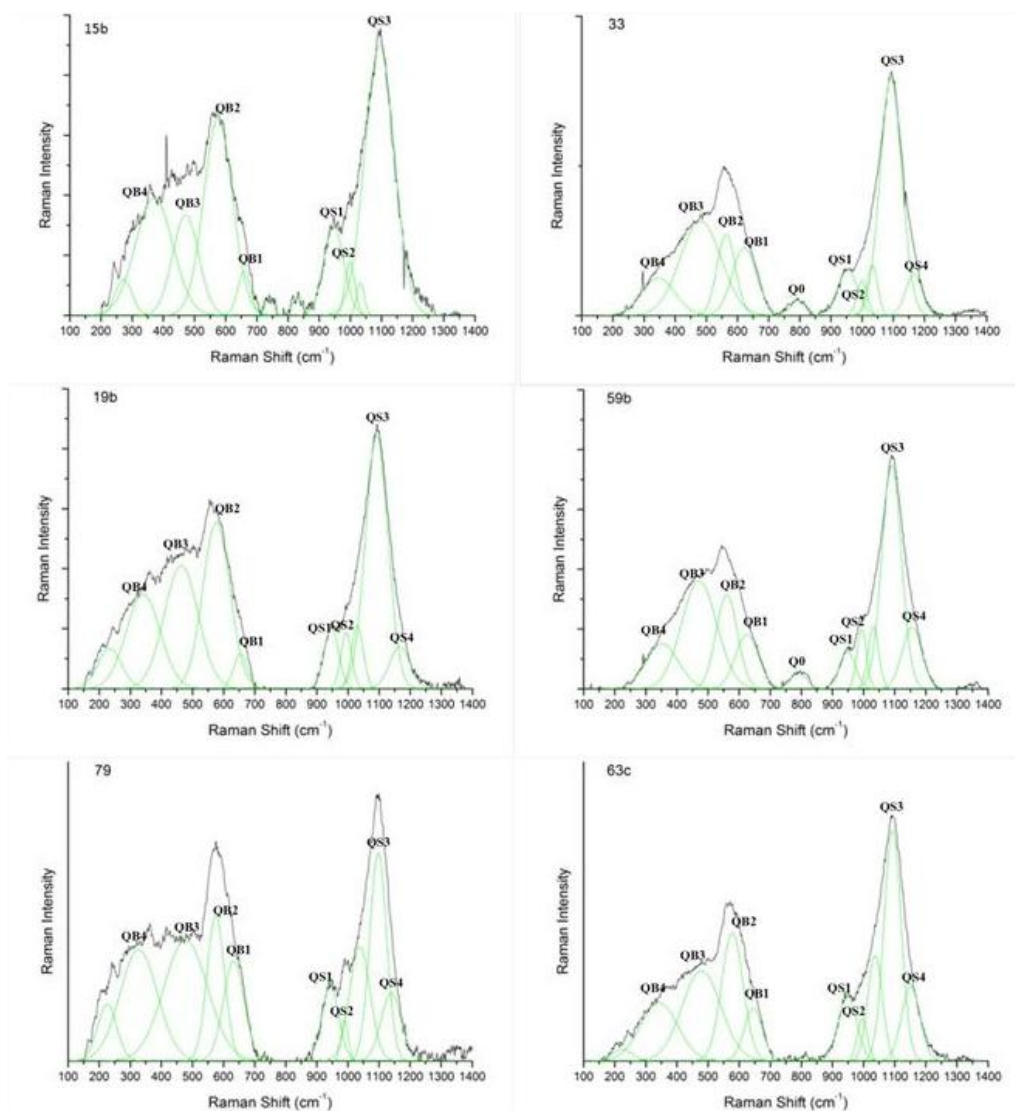


Figure 17. Deconvoluted Raman spectra of glass samples 15b, 19b, 79, 33, 59b, and 63c.

Maxima of Si-O bending (Q_S) and stretching (Q_B) Raman peaks and calculated I_p index values of the Olba glass samples are listed in Table 8. Bending and stretching maxima of the Olba glass samples are ranging from 560 to 583 cm^{-1} and from 1088 and 1097 cm^{-1} , respectively. The variation of peak maxima is due to the broad

character of these peaks and the resolution of the instrument ($\sim 9 \text{ cm}^{-1}$). Classification of historical/ancient glasses using the SiO_4 bending and stretching modes is shown in Figure 19 (Prinsloo et al., 2011). In Figure 18, the values of the Olba glass samples are also shown in yellow color. The majority of Olba glass samples are in the region assigned as Roman glasses and $\text{Na}_2\text{O}/\text{CaO}$ glasses. Glasses with bending band around 570 cm^{-1} are included in Roman and Chinese Cloisonné enamel (17th century) periods and their composition is close to 20% Na_2O and 8% CaO . Stretching peak (Q_{S3} -peak) maximum of the potash-rich glass is reported around 1105 cm^{-1} and for soda-rich glass, this Q_{S3} -peak is known to shift towards lower wavenumbers around 1090 cm^{-1} (Baert et al., 2011; Philippe Colomban, Etcheverry, et al., 2006; Prinsloo et al., 2011). Therefore, Olba glass samples can be classified as Na rich Soda-lime glasses since the average peak maxima values are 570 cm^{-1} and 1090 cm^{-1} corresponding to stretching and bending modes, respectively.

Table 8. Peak maxima values of Si-O bending (Q_{Bmax}), stretching (Q_{Smax}) peaks and I_p indexes of the 32 Olba glass samples.

Sample Code	Q_{Smax}, cm^{-1}	Q_{Bmax}, cm^{-1}	I_p index	Sample Code	Q_{Smax}, cm^{-1}	Q_{Bmax}, cm^{-1}	I_p index
12a	1093	575	1.4	4a	1093	582	1.8
14a	1093	571	1.3	52	1091	578	1.7
15b	1094	576	1.3	57a	1088	560	1.2
16a	1090	577	1.1	59b	1090	560	1.2
16b	1097	565	1.4	5a	1095	579	1.9
19b	1092	577	1.5	61a	1090	579	1.3
28	1091	581	1.3	61b	1090	579	1.4
29	1092	582	1.8	63c	1093	578	1.4
2a	1093	566	1.8	65a	1090	575	1.2
32	1090	582	1.2	6a	1092	583	1.6
33	1093	571	1.5	70a	1091	565	1.2
38a	1097	580	2.1	74a	1089	575	1.6
39	1093	579	1.8	78	1093	566	1.2
3a	1093	582	1.3	79	1097	575	2.2
43b	1093	582	2.0	7a	1092	573	1.4
46	1090	583	1.8	87b	1090	575	1.4

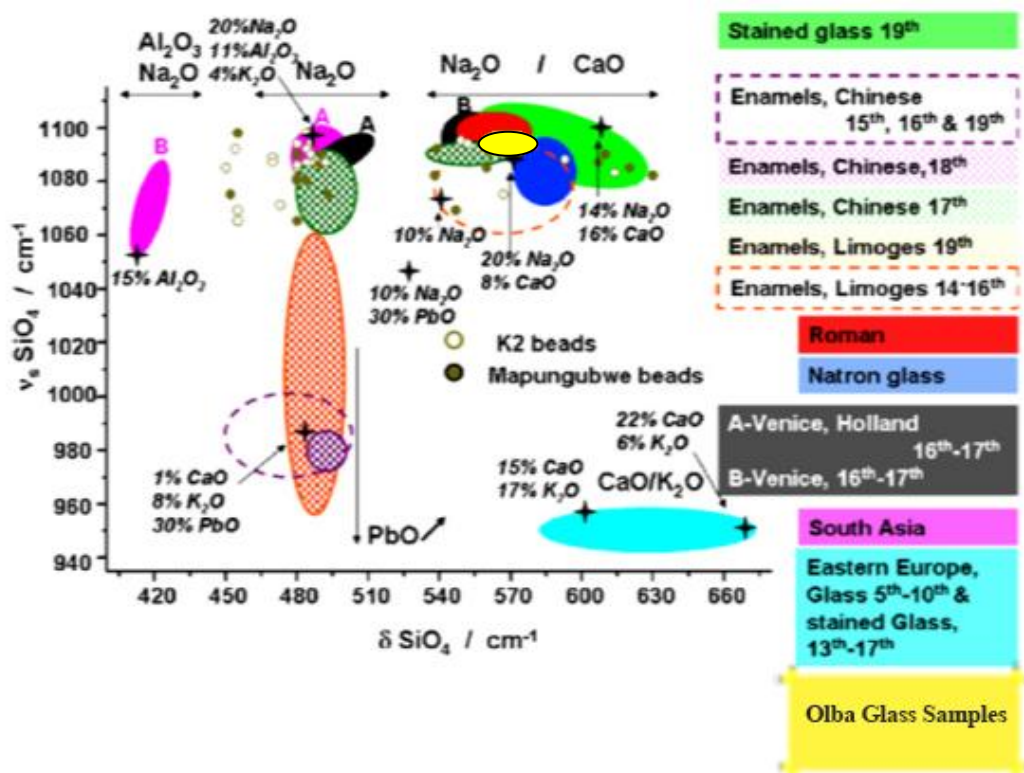


Figure 18. Classification of a variety of historical/ancient glasses using SiO_4 bending and stretching modes (Prinsloo et al., 2011). Olba glass results are also shown in yellow color. Adapted from “A Raman spectroscopic study of glass trade beads excavated at Mapungubwe hill and K2” by Colomban et al., 2011.

A graph of I_p vs. Q_{B2} values for some glass samples analyzed by Colomban^{13f} plus Olba glass samples are as shown in Figure 19. The Olba glass sample values overlap mostly with roman mosaics and Na_2O and $\text{Na}_2\text{O}+\text{K}_2\text{O}+\text{CaO}$ glass groups listed in Figure 19.

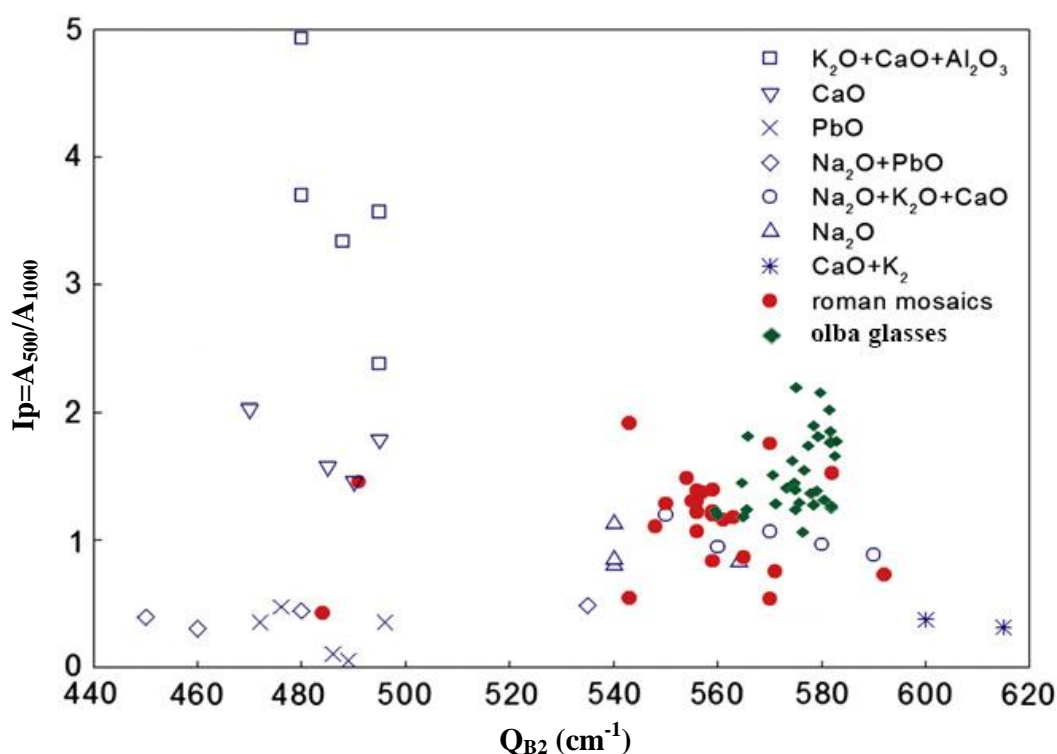


Figure 19. Polymerization index, I_p , vs. SiO_4 bending mode graph of various glass samples from the literature (Philippe Colomban & Tournié, 2007) plus Olba glass samples. Adapted from “On-site Raman identification and dating of ancient/modern stained glasses at the Sainte-Chapelle, Paris.” by Colomban et al., 2007.

An important classification of historical/ancient glasses and glazes was developed by Colomban and coworkers (Ph Colomban, 2004; Philippe Colomban, 2003b; Philippe Colomban, Tournie, et al., 2006; Ricciardi et al., 2009). They have distinguished so called seven glasses “families” by means of the parameters derived from their previous studies on ancient and historical glazes and glasses and 700 Raman spectra were collected from various glass samples. Principally, the relationship between the Raman index of polymerization, I_p , the glass composition and the processing temperature has been used to classify glasses into the seven groups as shown in Figure 20. Polymerization index is strongly correlated with the processing temperature ($\sim 1400^\circ\text{C}$ for $I_p \sim 7$, 1000°C for $I_p \sim 1$ and $\sim 600^\circ\text{C}$ or less for $I_p \sim 0.3$) (Ph Colomban, 2004).

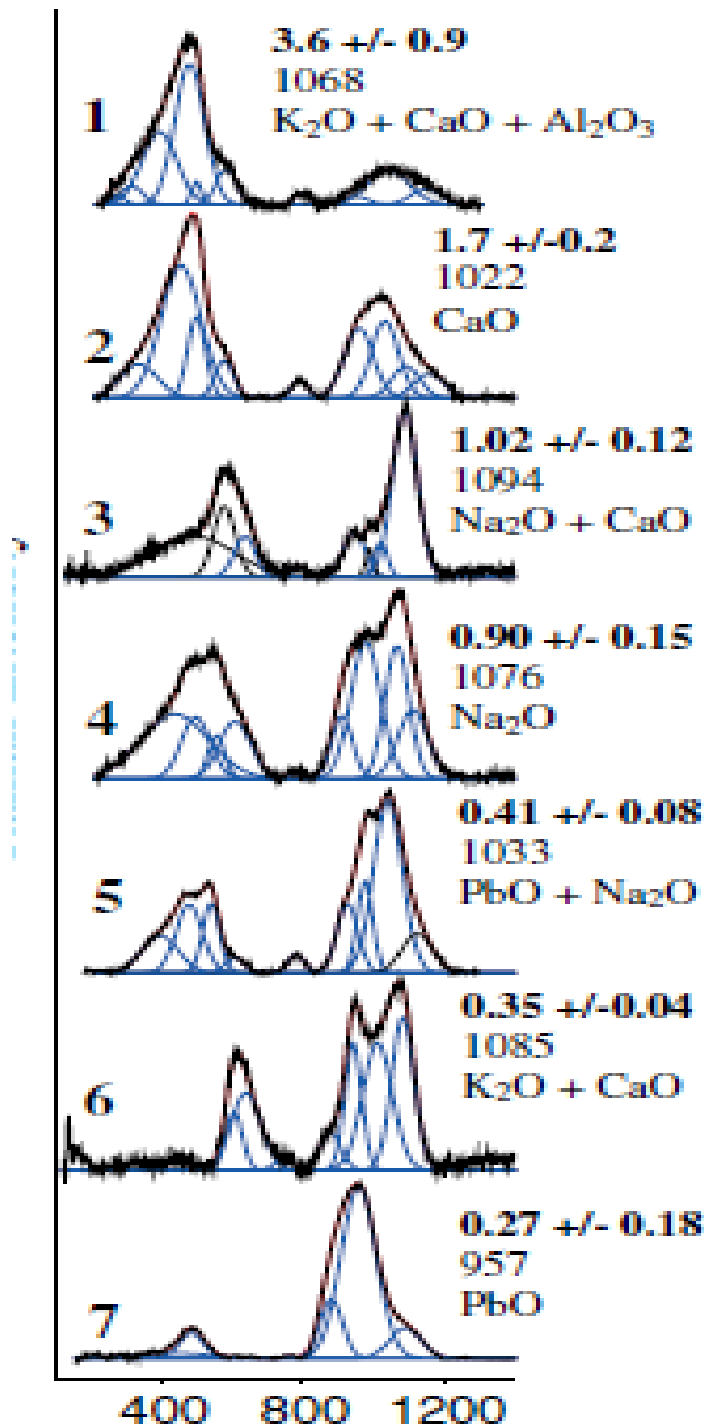


Figure 20 Representative examples of *seven glass families*. Polymerization index, glass type and stretching modes are indicated (Philippe Colomban, Tournie, & Bellot-Gurlet, 2006).

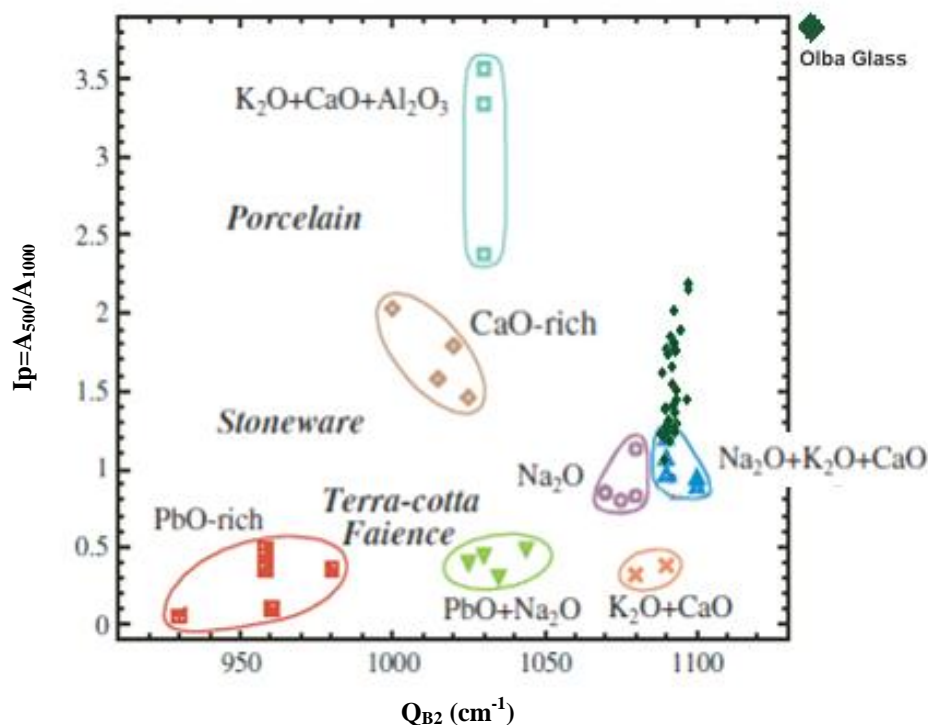


Figure 21. SiO₄ stretching mode vs. polymerization index, I_p, plot of a wide variety of glasses (Philippe Colomban & Tournié, 2007) plus Olba glass samples. Adapted from “On-site Raman identification and dating of ancient/modern stained glasses at the Sainte-Chapelle, Paris.” by Colomban et al., 2007.

I_p index values are calculated for the Olba glass samples using the formula derived by Colomban and coworkers (P. Colomban & Slodczyk, 2009) in this study. The calculated I_p values of the Olba glass samples are ranging from 1.1 to 2.2 (1.5±0.3). Therefore, it can be assumed that the processing temperature used for the Olba glass samples was around 1000 °C. Majority of I_p values of the Olba glass samples are between 1.0 and 2.0 and a few samples shows I_p values above 2.0 (43b, 38a, 79). As explained previously, these deviations in I_p values is due to the difficulties in calculation of I_p index values of the Olba glass samples having high background signal in their Raman spectrum. In conclusion, majority of the Olba glass samples fit into the *second and third families* in accordance with their I_p index values. However, stretching mode of the Olba glass samples (1092± 2 cm⁻¹) doesn't fit into the *second family* as seen in Figure 20.

Based upon the scheme presented in Figure 22, the Olba glass samples can be classified into the soda glass group with their low Pb levels (80 ± 52 ppm) and relatively high Na_2O levels (8.9 ± 2) (Baert et al., 2011). Furthermore, when relatively low concentration of potassium and magnesium is considered (K_2O and $\text{MgO} < 1.5\%$ each), they are most probably produced using natron instead of plant ashes. If natron is the soda source of soda-lime type ancient glasses, they are expected to contain 4–9% CaO and 12–23% Na_2O (Ricciardi et al., 2009). Similarly, 65–70%, SiO_2 , 2.5% Al_2O_3 , 0.5% Fe_2O_3 and 0.5% MnO_2 values are accepted as typical for ancient soda-lime glass. The composition of the Olba glass samples as listed in Table 5 is inside these levels for SiO_2 , Al_2O_3 , Fe_2O_3 and MnO_2 therefore, the Olba glasses can be classified as soda-lime glass based on these results. However, SiO_2 , Na_2O and Al_2O_3 concentrations of Olba glass samples are lower than expected for a natron type Roman soda-lime-silica glass {Janssens, 2013 #75}. These low results are probably effect the I_p index value calculated using SiO_4 stretching and bending modes.

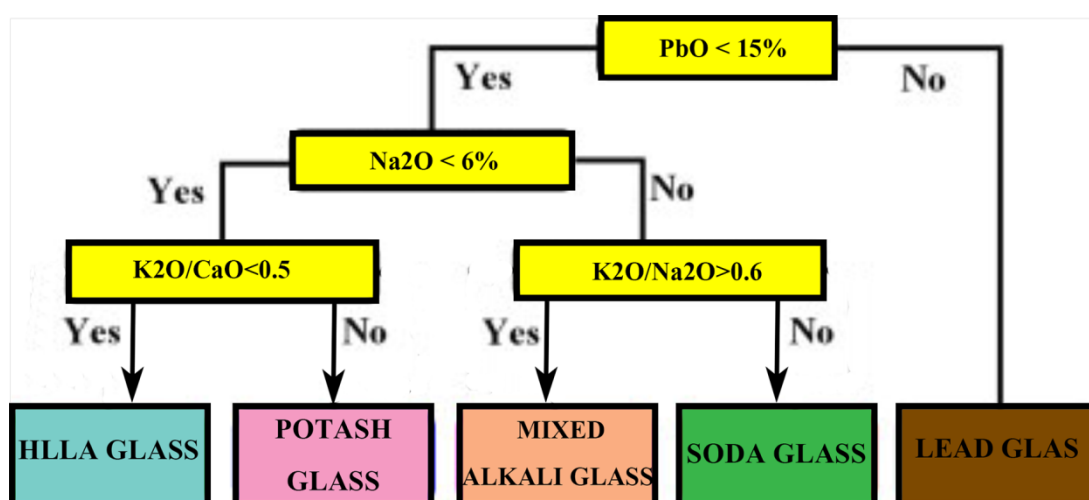


Figure 22 Classification of window glass fragments based on their major composition (Baert et al., 2011).

The Raman spectrum is known to originate from the molecular vibrations of the molecular bonds. The continuous curve shaped Raman spectrum of glasses can thus be deconvoluted into several separate peaks, each of which corresponds to the Raman scattering contribution from a vibrational molecular bond. The spectra of the

Olba glasses were deconvoluted into 3 major peaks at 320, 497 and 595 cm^{-1} for the bending mode and 952, 991 and 1092 cm^{-1} for the stretching modes (Prinsloo et al., 2011; Tournié et al., 2012; Ricciardi et al., 2009). Band positions and assignments of each deconvoluted peak are given in Table 9.

Table 9. Band positions and assignments of the various peaks within the Olba glass composition.

Component	Band Positions (cm^{-1})
Q_{B4}	312-387
Q_{B3}	457-491
Q_{B2}	560-583
Q_{B1}	621-660
Q_0	787-818
Q_{S1}	939-953
Q_{S2}	989-1005
Q_{S3}	1088-1097
Q_{S4}	1137-1198
I_p	1.1-2.2

The bending mode of a typical soda-lime glass is at the wavenumber 595 cm^{-1} (Q_{B2}) (Prinsloo et al., 2011; Ricciardi et al., 2009; Tournié et al., 2012) however, a shift to lower wavenumbers is measured at 575 cm^{-1} for the Olba glass samples. The main difference between Olba glasses and typical soda glasses is lower Al_2O_3 , SiO_2 , Na_2O concentration of Olba glass samples compared to soda glasses. Therefore, the correlation between Q_{B2} and the concentration of Al_2O_3 , SiO_2 , Na_2O in Olba glasses are studied in detail.

However, no bivariate correlation is found between these variables. Among Al_2O_3 , SiO_2 and Na_2O , only Fe_2O_3 is significantly correlated with Q_{B2} at the level of 0.01 as shown in shown in Table 10.

Table 10. Correlation between Fe₂O₃, Na₂O, Al₂O₃, SiO₂ concentration and Q_{B2} values.

		Fe ₂ O ₃	Na ₂ O	Al ₂ O ₃	SiO ₂	Q _{B2}
Fe ₂ O ₃	Pearson Correlation	1	0.363*	0.174	0.026	0.620**
	Sig. (2-tailed)		0.035	0.326	0.883	0.000
	N	34	34	34	34	32
Na ₂ O	Pearson Correlation	0.363*	1	0.459**	0.602**	0.152
	Sig. (2-tailed)	0.035		0.006	,000	0.407
	N	34	34	34	34	32
Al ₂ O ₃	Pearson Correlation	0.174	0.459**	1	0.717**	0.084
	Sig. (2-tailed)	0.326	0.006		,000	0.648
	N	34	34	34	34	32
SiO ₂	Pearson Correlation	0.026	0.602**	0.717**	1	-0.169
	Sig. (2-tailed)	0.883	0.000	0.000		0.354
	N	34	34	34	34	32
Q _{B2}	Pearson Correlation	0.620**	0.152	0.084	-0.169	1
	Sig. (2-tailed)	0.000	0.407	0.648	0.354	
	N	32	32	32	32	32

*. Correlation is significant at the 0.05 level (2-tailed).

**. Correlation is significant at the 0.01 level (2-tailed).

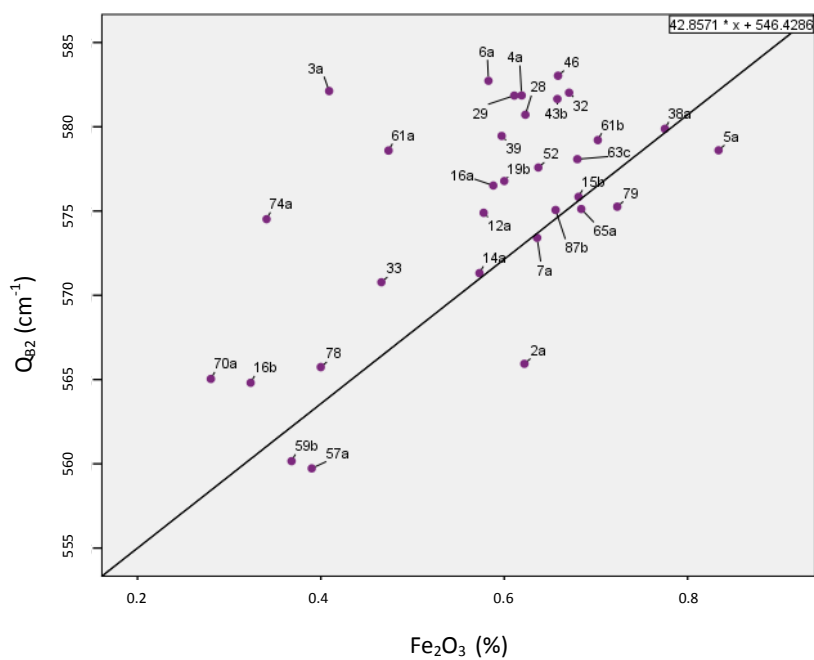


Figure 23. Q_{B2} values vs. Fe₂O₃ concentration of the Olba glass samples.

The bending mode of a typical soda-lime silica glass is reported as 595 cm^{-1} as we discussed in previous sections^{14j, 14m, 14n}. When the line equation shown in Figure 23 is used to determine the concentration of Fe_2O_3 at 595 cm^{-1} , 1.1% is calculated. Nevertheless, the highest Fe_2O_3 concentration measured from Olba glass samples is as 0.8%. Therefore, low Fe_2O_3 concentration in Olba glass samples may be the reason of getting lower Q_{B2} values compared to soda-lime silica glasses.

Cesaratto and coworkers were able to determine the concentration of Pb in glass by using the peak maxima of the stretching mode (Cesaratto et al., 2010). Nevertheless, Pb concentrations of the Olba glasses are at ppm level and we could not find such correlation between the concentration of Pb and the peak maxima of stretching mode. On the other hand, Pb concentration of the Olba glass samples show a positive correlation with I_p index values as shown in Figure 24. It is known that lead oxide may act as a stabilizer, flux or vitrifier (Janssens, 2013). Thus higher I_p index value indicates a stronger glass network, being positively correlated with I_p index values, lead could play a role as vitrifier in Olba glass samples. Pb concentration is also positively correlated with MnO concentration shown in Figure 25.

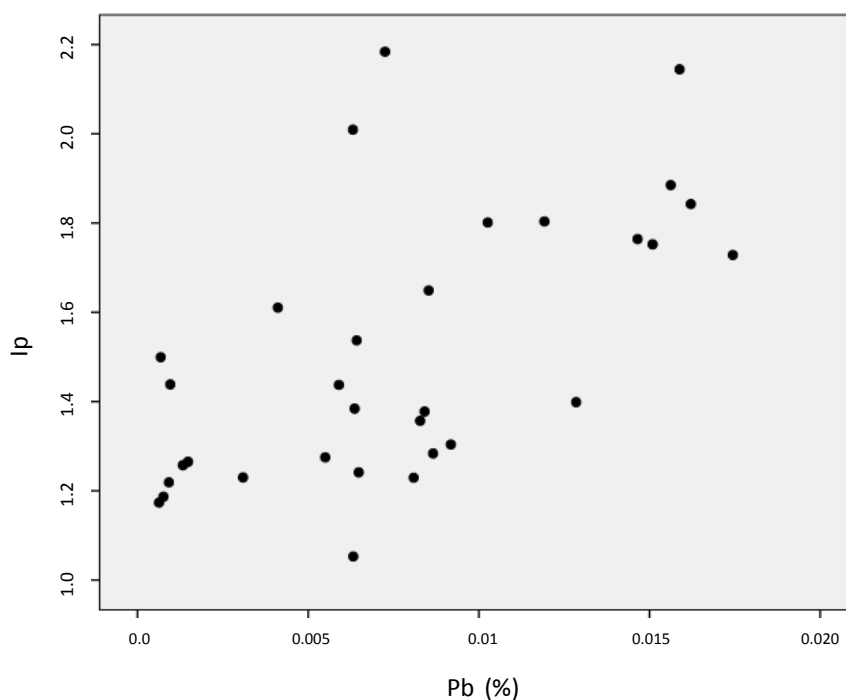


Figure 24. The scatter plot of I_p index vs. Pb concentration of 32 Olba glass samples.

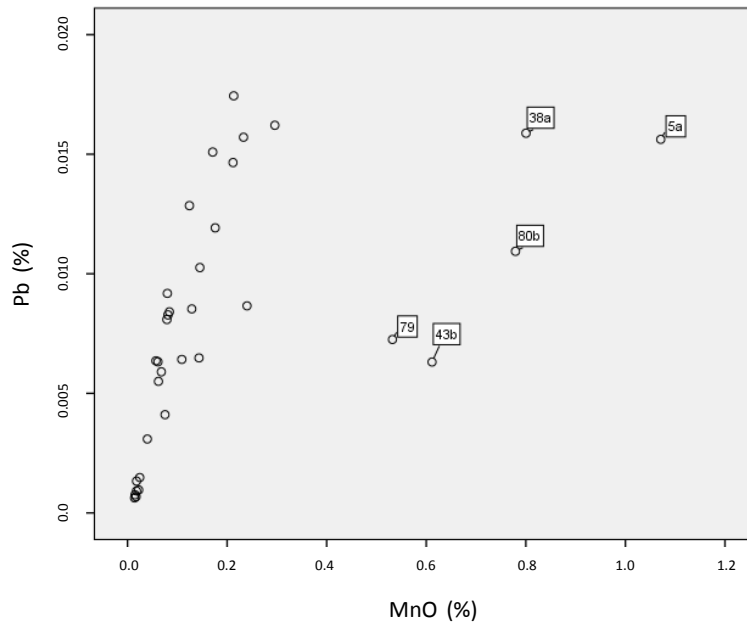


Figure 25. The scatter plot of Pb concentration vs. MnO concentration of 34 Olba glass samples.

CHAPTER 5

CONCLUSION

A number of glass fragments obtained from the excavations of Mersin Olba archaeological site was studied by Raman spectroscopy and polarized energy dispersive XRF methods.

Outcomes of the Raman spectroscopy enabled us to classify the sample group as soda rich soda-lime type glasses in accordance with their I_p , Q_{S3} and Q_{B2} values. Raman spectrometry analyses also confirm that samples were fired at temperatures above 1000° C according to the I_p values between 1.0 and 2.0. According to the classification of historical/ancient glass and glazes introduced and developed by Colomban and coworkers by means of the Raman index of polymerization, majority of our samples fit into the third family and some glasses can be considered as the member of the second family. It is observed that samples giving high background signal have a broader bending band in their Raman spectrum. Hence, their polymerization indexes are higher than the ones with lower background signal. Therefore, it is assumed that a defect arising from the inadequate base-subtraction/deconvolution process could be a reason for higher I_p index values. Also a strong positive correlation among MnO and Pb shows that MnO and Pb can be the possible cause of relatively high I_p index values.

The results given by PED-XRF are revealed that chemical compositions of Olba glass samples are very similar. All samples is found to be soda-lime-silica glasses containing SiO_2 as the former, Na_2O as the fluxing agent, and CaO as the stabilizer. Correlation analyses among SiO_2 , Fe_2O_3 and TiO_2 have showed that; probable source of iron and titanium in samples 16b, 74a, 70a, 33, 80b, 3a, 57a, 59b, 78 and 61a was silica source. However, for samples 12a, 14a, 15b, 16a, 19b, 28, 29, 2a, 32,

38a, 39, 43b, 46, 4a, 52, 5a, 61b, 63c, 65a, 6a, 79, 7a, 80b, 84b and 87b, besides Fe_2O_3 introduced by silica source, there might have been a second source of Fe_2O_3 . This additional source could be one of the raw materials or a contamination arising from glassmaking procedures. Therefore, existence of two different glassmaking procedures for two groups can be argued.

The potash and magnesia concentration of the Olba glass samples are both less than 1% and P_2O_5 concentration is less than 0.1%. These results are compared with the literature data and discussed in detail in previous sections and it is concluded that soda source of Olba glass samples is mainly natron. Positive cross correlation between concentration of SiO_2 , Al_2O_3 and CaO indicates that Al_2O_3 and CaO were added to the Olba glass samples together with the silica source.

Concentration of alumina concentration in natron is very low, thus considering the strong possibility that Al_2O_3 is introduced into glass samples along with silica, low Al_2O_3 content of Olba glass samples suggest that a mature (relatively pure) sand source was used as the silica source. CaO incorporated with sand is generally thought to be originating from shell fragments or eroded limestone. Furthermore, high strontium and low zirconium levels detected in Olba glass samples imply coastal sand usage.

High MnO concentration of samples 12a, 14a, 15b, 16a, 19b, 28, 29, 2a, 32, 38a, 39, 43b, 46, 4a, 52, 5a, 61b, 63c, 65a, 6a, 79, 7a, 80b, 84b and 87b indicates the intentional use of MnO. Positive correlation between Fe_2O_3 and MnO for these samples shows that Fe_2O_3 and MnO might share the same source.

REFERENCES

Baert, K., Meulebroeck, W., Wouters, H., Ceglia, A., Nys, K., Thienpont, H., & Terryn, H. , 2011, Raman Spectroscopy as a Rapid Screening Method for Ancient Plain Window Glass, *Journal of Raman Spectroscopy*, 42(5), 1055-1061

Beşer, Elif., 2009, Archaeometrical Investigation Of Some Medieval Glass Samples From Alanya Region, (The Degree Of Master Of Science In Archaeometry), Middle East Technical University, Ankara.

Bouchard, M., Smith, D. C., & Carabatos-Nedelec, C., 2007, An Investigation of the Feasibility of Applying Raman Microscopy for Exploring Stained Glass, *Spectrochim Acta A Mol Biomol Spectrosc*, 68(4), 1101-1113

Brems, D., & Degryse, P., 2014, Trace Element Analysis in Provenancing Roman Glass-Making, *Archaeometry*, 56, 116-136

Brems, Dieter, Degryse, Patrick, Hasendoncks, Femke, Gimeno, Domingo, Silvestri, Alberta, Vassilieva, Honings, Johan, 2012, Western Mediterranean Sand Deposits as a Raw Material for Roman Glass Production, *Journal of Archaeological Science*, 39(9), 2897-2907

Brill, R.H., 1999, *Chemical Analyses of Early Glasses: The Tables (Vol. Volume 2)*, New York

Brill, R.H., 1999, *Chemical Analyses of Early Glasses: The Catalogue (Vol.1)*, Corning Museum of Glass, New York

Brooke, C. J., Edwards, H. G. M., & Tait, J. K. F., 1999, The Bottesford Blue Mystery: A Raman Spectroscopic Study Of Post-Mediaeval Glazed Tiles, *Journal of Raman Spectroscopy*, 30(6), 429-434

Caddy, Brian, 2001, *Forensic Examination of Glass and Paint Analysis and Interpretation*, Taylor & Francis, London

Cesaratto, A., Sichel, P., Bersani, D., Lottici, P. P., Montenero, A., Salvioli-Mariani, E., & Catarsi, M., 2010, Characterization of Archeological Glasses by Micro-Raman Spectroscopy, *Journal of Raman spectroscopy*, 41(12), 1682-1687

Colomban, P., & Slodczyk, A., 2009, Raman Intensity: An Important Tool in the Study of Nanomaterials and Nanostructures, *Acta Physica Polonica A*, 116(1), 7-12

Colomban, Ph., 2004, Raman Spectrometry, A Unique Tool to Analyze and Classify Ancient Ceramics and Glasses, *Applied Physics A: Materials Science & Processing*, 79(2), 167-170

Colomban, Ph., & Treppoz, Françoise, 2001, Identification and Differentiation of Ancient and Modern European Porcelains by Raman Macro and Micro-spectroscopy, *Journal of Raman Spectroscopy*, 32, 93–102

Colomban, Philippe., 2003a, Lapis lazuli As Unexpected Blue Pigment In Iranian Lijvardina Ceramics, *Journal of Raman Spectroscopy*, 34(6), 420-423

Colomban, Philippe, 2003b, Polymerization Degree and Raman Identification of Ancient Glasses Used For Jewelry, Ceramic Enamels and Mosaics, *Journal of Non-Crystalline Solids*, 323(1-3), 180-187

Colomban, Philippe, 2008, On-site Raman identification and dating of ancient glasses: A review of procedures and tools. *Journal of Cultural Heritage*, 9, e55-e60

Colomban, Philippe, Etcheverry, Marie-Pierre, Asquier, Magali, Bounichou, Mathieu, & Tournié, Aurélie., 2006, Raman Identification of Ancient Stained Glasses and Their Degree of Deterioration, *Journal of Raman Spectroscopy*, 37(5), 614-626

Colomban, Philippe, Milande, Véronique, & Le Bihan, Lionel., 2004, On-site Raman Analysis of Iznik Pottery Glazes and Pigments, *Journal of Raman Spectroscopy*, 35(7), 527-535

Colomban, Philippe, & Paulsen, Ove., 2005, Non-Destructive Determination of the Structure and Composition of Glazes by Raman Spectroscopy, *Journal of the American Ceramic Society*, 88(2), 390-395

Colomban, Philippe, Sagon, Gerard, & Faurel, Xavier, 2001, Differentiation of Antique Ceramics from the Raman Spectra of Their Coloured Glazes and Paintings, *Journal of Raman Spectroscopy*, 32(5), 351-360

Colomban, Philippe, Tournie, Aurelie, & Ricciardi, Paola., 2009, Raman Spectroscopy of Copper Nanoparticle-Containing Glass Matrices: Ancient Red Stained-Glass Windows, *Journal of Raman Spectroscopy*, 40(12), 1949-1955

Colomban, Philippe, & Tournié, Aurélie., 2007, On-site Raman Identification and Dating of Ancient/Modern Stained Glasses at the Sainte-Chapelle, Paris. *Journal of Cultural Heritage*, 8(3), 242-256

Colomban, Philippe, Tournie, Aurélie, & Bellot-Gurlet, Ludovic., 2006, Raman Identification of Glassy Silicates Used in Ceramics, Glass and Jewellery: A Tentative Differentiation Guide, *Journal of Raman Spectroscopy*, 37(8), 841-852

Davison, S., 2003, *Conservation and Restoration of Glass* (Second ed.), Elsevier Ltd Great Britain

Smith, E., Dent, G., 2005, *Modern Raman Spectroscopy A Practical Approach*, John Wiley & Sons Ltd, England

Durukan, Murat, 2005, Monumental Tomb Forms in the Olba Region. *Anatolian Studies*, 55, 107-126.

Edwards, Howell G. M., Vandenabeele, Peter, 2012, *Analytical Archaeometry Selected Topics*, The Royal Society of Chemistry, United Kingdom

Erten, Emel, 2003, Glass Finds from Olba Survey – 2001, *OLBA VII*, 145-154.

Erten, Emel, 2007, Surveys in Mersin - Silifke - Olba in 2006, *ANMED 5*, 133-136

Fernandes, Paula, Vilarigues, Márcia, Alves, Luís C., & da Silva, Rui C., 2008, Stained Glasses from Monastery of Batalha: Non-destructive Characterization of Glasses and Glass Paintings, *Journal of Cultural Heritage*, 9, e5-e9

Floudas, George, Paluch, Marian, Grzybowski, Andrzej, & Ngai, K.L., 2011, *Molecular Dynamics of Glass-Forming Systems*, Springer-Verlag, Berlin

Freestone, I. C., Leslie, K. A., Thirlwall, M., 2003, Strontium Isotopes in the Investigation of Early Glass Production: Byzantine and Early Islamic Glass from the Near East, *Archaeometry*, 45(1), 19-32.

Galli, S., Mastelloni, M., Ponterio, R., Sabatino, G., & Triscari, M., 2004, Raman and Scanning Electron Microscopy and Energy-Dispersive X-Ray Techniques for the Characterization of Colouring and Opacifying Agents in Roman Mosaic Glass Tesserae, *Journal of Raman Spectroscopy*, 35(89), 622-627

Greiff, Susanne, Schuster, Jan., 2008, Technological Study Of Enamelling on Roman Glass: The Nature of Opacifying, Decolourizing and Fining Agents Used With the

Glass Beakers from Lübsow (Lubieszewo, Poland), *Journal of Cultural Heritage*, 9, e27-e32.

Henderson, Jullian., 2013, *Ancient Glass an Interdisciplinary Exploration*, Cambridge University Press, United States of America

Jackson, C. M., 2005, *Making Colourless Glass in The Roman Period*, *Archaeometry*, 47

Janssens, K., 2013, *Modern Methods for Analysing Archaeological and Historical Glass (Vol. 1)*, JohnWiley & Sons, Ltd, United Kingdom

Larkin, P., 2011, *Infrared and Raman Spectroscopy Principles and Spectral Interpretation*, Elsevier Inc, USA

Lewis, Ian R., & Edwards, Howell G. M., 2001, *Hanbook of Raman Spectroscopy*, Taylor & Francis, New York

Pollard M. A., Heron C., 2008, *Archaeological Chemistry (Second Edition)*, The Royal Society of Chemistry, Cambridge

McIntosh, C., Toulouse, J., & Tick, P., 1997, *The Boson Peak in Alkali Silicate Glasses*. *Journal of Non-Crystalline Solids*

Nguyen Quang Liem, Gerard Sagon, Vu Xuan Quang, Ha Van Tan, Philippe Colomban., 2000, *Raman Study of the Microstructure, Composition and Processing of Ancient Vietnamese (Proto) Porcelains and Celadons (13–16th centuries)*. *Journal of Raman Spectroscopy*, 31, 933–942

Oikonomou, Ar, Triantafyllidis, P., Beltsios, K., Zacharias, N., & Karakassides, M., 2008, Raman Structural Study of Ancient Glass Artefacts from the Island of Rhodes, *Journal of Non-Crystalline Solids*, 354(2-9), 768-772

Prinsloo, Linda C., Tournié, Aurélie, & Colomban, Philippe, 2011, A Raman Spectroscopic Study of Glass Trade Beads Excavated at Mapungubwe Hill And K2, Two Archaeological Sites in Southern Africa, Raises Questions About the Last Occupation Date of the Hill, *Journal of Archaeological Science*, 38(12), 3264-3277

Raffaëly, L., Champagnon, B., Ollier, N., & Foy, D., 2008, IR and Raman Spectroscopies, a Way to Understand How the Roman Window Glasses Were Made?, *Journal of Non-Crystalline Solids*, 354(2-9), 780-786

Rao, K. J., 2002, *Structural Chemistry of Glasses*, Elsevier Science & Technology Books

Raškovska, A., Minčeva-Šukarova, B., Grupče, O., & Colomban, Ph., 2009, Characterization of Pottery from Republic of Macedonia II. Raman and Infrared Analyses of Glazed Pottery Finds from Skopsko Kale, *Journal of Raman Spectroscopy*

Rasmussen, Seth C., 2012, *How Glass Changed the World*, Springer, London

Ricci, Camilla, Miliani, Costanza, Rosi, Francesca, Brunetti, Brunetto G., & Sgamellotti, Antonio., 2007, Structural Characterization of the Glassy Phase in Majolica Glazes by Raman Spectroscopy: A Comparison Between Renaissance Samples and Replica Processed at Different Temperatures, *Journal of Non-Crystalline Solids*, 353(11-12), 1054-1059

Ricciardi, Paola, Colomban, Philippe, Tournié, Aurélie, & Milande, Véronique, 2009, Nondestructive On-Site Identification of Ancient Glasses: Genuine Artefacts, Embellished Pieces or Forgeries, *Journal of Raman Spectroscopy*, 40(6), 604-617

Robinet, Laurianne, Coupry, Claude, Eremin, Katherine, & Hall, Christopher, 2006, The Use of Raman Spectrometry to Predict the Stability of Historic Glasses, *Journal of Raman Spectroscopy*, 37(7), 789-797

Robinet, Laurianne, Eremin, Katherine, Coupry, Claude, Hall, Christopher, & Lacome, Nelly, 2007, Effect of Organic Acid Vapors on the Alteration of Soda Silicate Glass, *Journal of Non-Crystalline Solids*, 353(16-17), 1546-1559

Robinet, Laurianne, Hall, Christopher, Eremin, Katherine, Fearn, Sarah, & Tate, Jim, 2009, Alteration of Soda Silicate Glasses by Organic Pollutants in Museums: Mechanisms and Kinetics, *Journal of Non-Crystalline Solids*, 355(28-30), 1479-1488

Šesták, Jaroslav, Mareš, Jiří J., & Hubík, Pavel, 2011, *Glassy, Amorphous and Nano-Crystalline Materials Thermal Physics, Analysis, Structure and Properties*, Springer, New York

Shelby, J. E., 2005, *Introduction to Glass Science and Technology (Second Edition)*, The Royal Society of Chemistry

Shortland, Andrew, Schachner, Lukas, Freestone, Ian, & Tite, Michael, 2006, Natron as a Flux in the Early Vitreous Materials Industry: Sources, Beginnings and Reasons for Decline, *Journal of Archaeological Science*, 33(4), 521-530

Simsek, G., Colomban, Philippe, & Milande, Véronique, 2009, Tentative Differentiation Between Iznik Tiles and Copies with Raman Spectroscopy Using both Laboratory and Portable Instruments, *Journal of Raman Spectroscopy*, 41(5), 529-536

Tanevska, Vinka, Colomban, Philippe, Minčeva-Šukarova, Biljana, & Grupče, Orhideja, 2009, Characterization of Pottery from the Republic of Macedonia I: Raman Analyses of Byzantine Glazed Pottery Excavated from Prilep and Skopje (12th-14th centuries), *Journal of Raman Spectroscopy*, 40(9), 1240-1248

Tournié, Aurélie, Prinsloo, Linda C., & Colomban, Philippe., 2012, Raman Classification of Glass Beads Excavated on Mapungubwe Hill and K2, Two Archaeological Sites in South Africa, *Journal of Raman Spectroscopy*, 43(4), 532-542

Towle, A. C., 2002, a Scientific and Archaeological Investigation of Prehistoric Glasses from Italy, Doctor of Philosophy, University of Nottingham

Vandenabeele, P., Edwards, H. G., & Jehlicka, J., 2014, The Role of Mobile Instrumentation in Novel Applications of Raman Spectroscopy, *Archaeometry, Geosciences, and Forensics* Vol. 43

Welter, N., Schüssler, U., & Kiefer, W., 2007, Characterization of Inorganic Pigments in Ancient Glass Beads by Means of Raman Microspectroscopy, Microprobe Analysis and X-ray Diffractometry, *Journal of Raman Spectroscopy*, 38(1), 113-121

Won-in, K., Thongkam, Y., Pongkrapan, S., Intarasiri, S., Thongleurm, C., Kamwanna, T., Dararutana, P., 2011, Raman Spectroscopic Study on Archaeological Glasses in Thailand: Ancient Thai Glass, *Spectrochim Acta A Mol. Biomol. Spectrosc.*, 83(1), 231-235

APPENDIX A.

OPTICAL IMAGES OF THE OLBA GLASS SAMPLES

Table A.1.

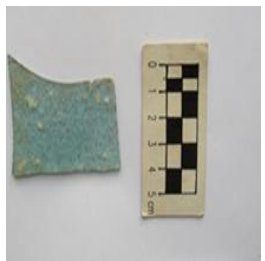
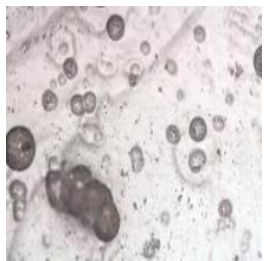
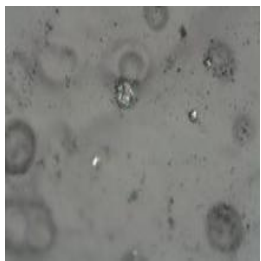





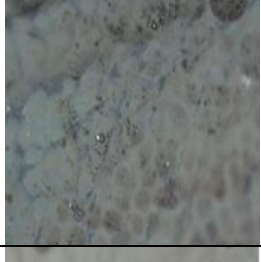

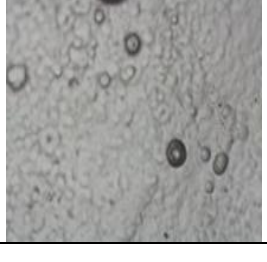

Sample	1:1 scaled	Under 20X O. Microscope	Under 50X O. Microscope
12a			
16b			
29			
32			

Table A.1. continued


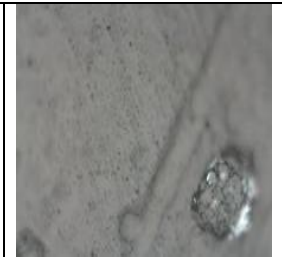

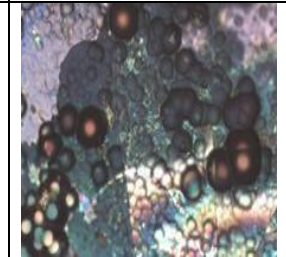
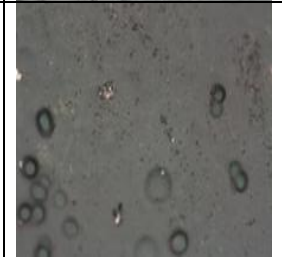

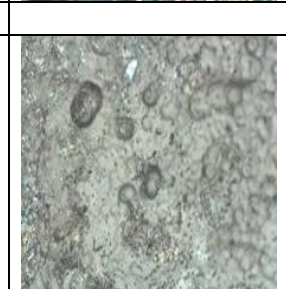
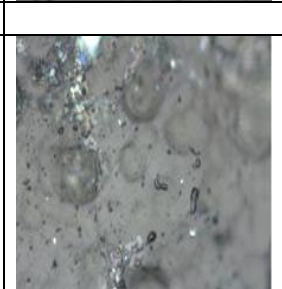

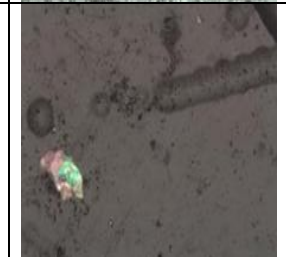
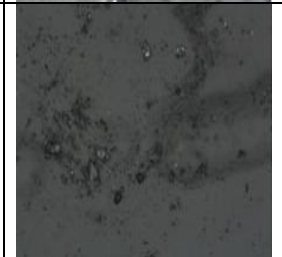

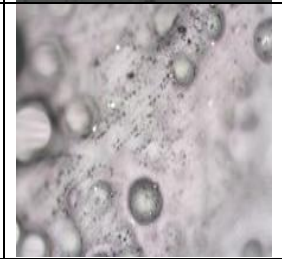
28			
57a			
61b			
70			
87			

Table A.1. continued



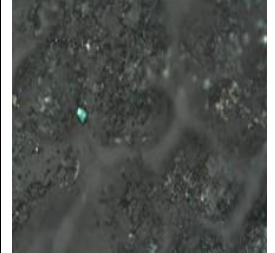

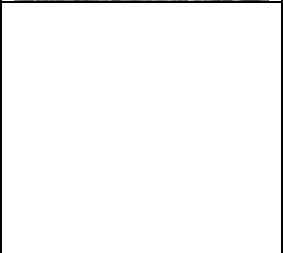


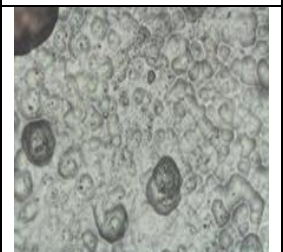


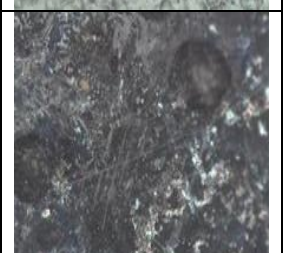
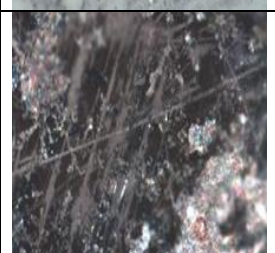

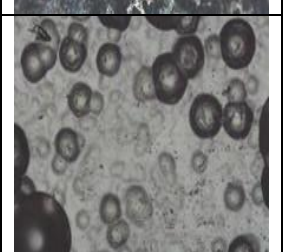
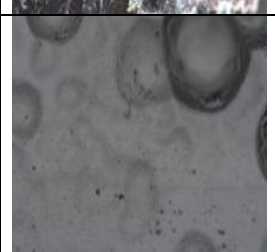

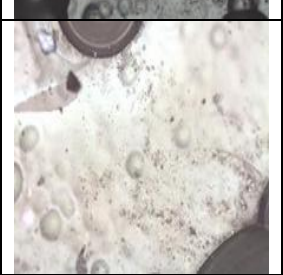

33			
38a			
39			
43b			
46			
5a			

Table A.1. continued


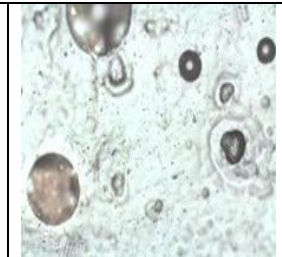
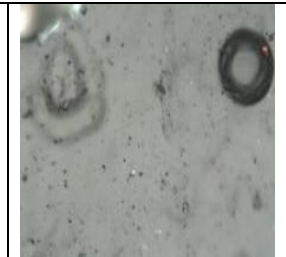

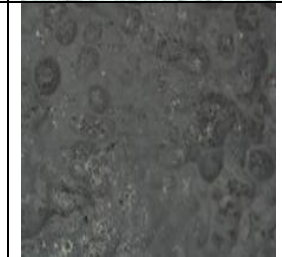
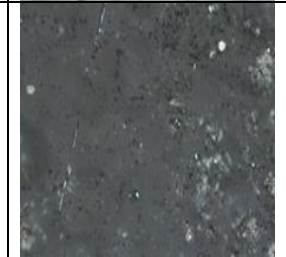


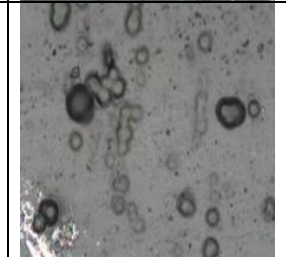

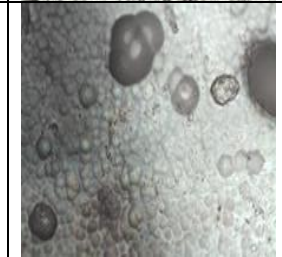
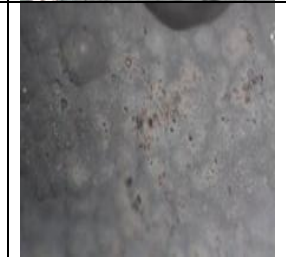

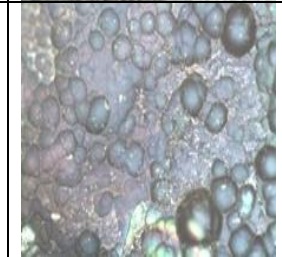


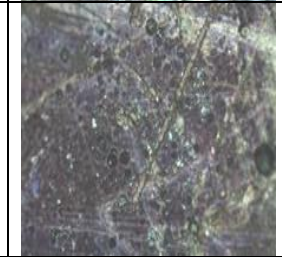
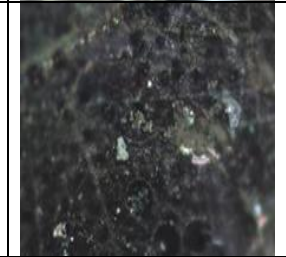
52			
6a			
61a			
63c			
65a			
7a			

Table A.1. continued


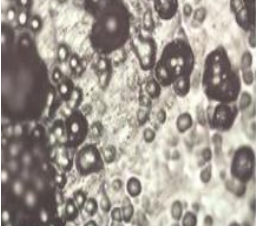







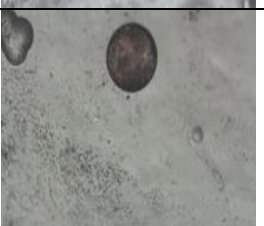








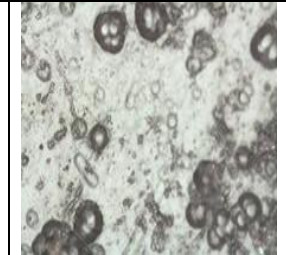
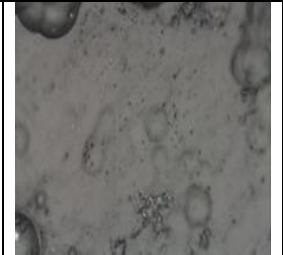

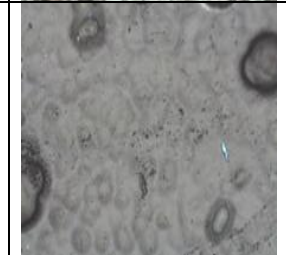


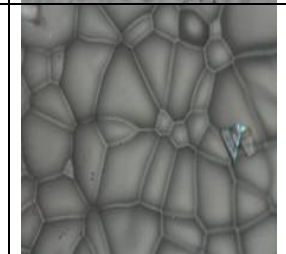
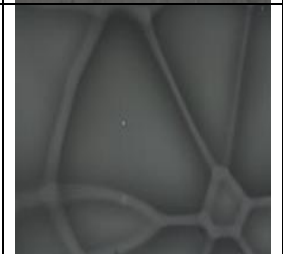

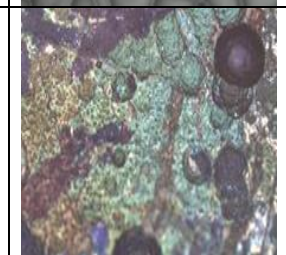
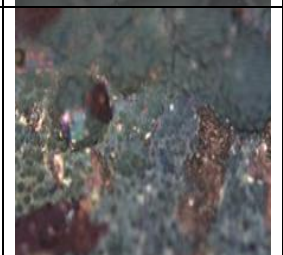

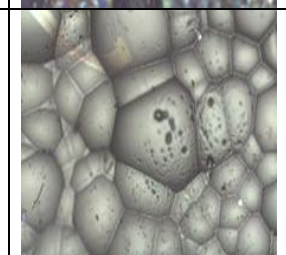
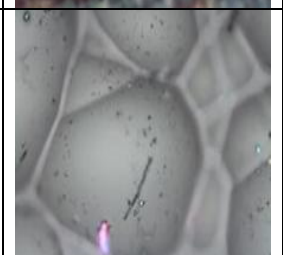

2a			
4a			
14a			
15b			
16a			
19b			

Table A.1. continued

74a			
78			
79			
80b			
84b			
3a			

APPENDIX B.

THICKNESSES OF THE OLBA GLASS SAMPLES

Table B.1.

Sample Code	Thickness (mm)
12a	0.2-0.21
14a	0.345- 0.29
15b	1.15 (amorf)
16a	0.22
16b	0.29-0.3
19b	0.175-0.18
28	0.295-0.315
29	0.375- 0.495
2a	0.37-0.38
32	0.375-0.45
33	0.355
38a	0.56-0.595
39	0.26
3a	0.29-0.24
43b	0.430-0.435
46	0.36-0.41
4a	0.3-0;38
52	0.545-0.515
57a	0.46-0.36
59b	0.325- 0;24
5a	0.28-0.21
61a	0.43-0.36

Table B.1. continued

61b	0.265-0.245
63c	0.32-0.29
65a	0.3-0.24
6a	0.27
70a	0.25-0.23
74a	0.23-0.2
78	0.375-0.25
79	0.31-0.12
7a	0.35-0.22
80b	0.4-0.42
84b	0.29-0.275
87b	0.35-0.29

APPENDIX C.

ELEMENTAL COMPOSITIONS OF THE OLBA GLASS SAMPLES

Table C.1. Elemental Compositions (ppm)

Element	4a	46	43b	3a	39	38a	33	32	2a	29	28	19b	16b	16a	15b	14a	12a
Co	17.5	11.4	9.8	19.4	11.3	22.7	17.6	12.7	8.4	26	19.3	9.4	16.5	11.8	9.8	7.5	14.5
Ni	12.8	10.3	8.7	5.6	10.6	11.6	5.5	12.7	8.6	9.2	9.9	8.9	4.9	9.2	10.8	8.8	5.8
Cu	82.3	60.5	29.3	4.6	69.2	73.8	1.6	74.6	68.8	73.8	63.1	47.8	6.3	29.4	36.7	32.2	32.2
Zn	9.1	12.3	11.8	6	9.3	13.3	7.1	14	12.2	10.5	10.8	8.9	5.2	9.4	12.8	8.7	7.9
Ga	1.4	3.1	4	3.5	2.3	2.4	3.4	4.6	3.3	2.6	2.8	3.1	4.4	4.2	3.2	5.2	3.5
Ger	0.6	0.6	1.2	0.6	0.5	0.6	0.6	0.8	0.6	0.6	0.6	0.6	0.6	0.6	0.7	0.6	0.5
As	2.6	2.6	3.4	1.3	2.1	3.5	1.7	1.7	2.3	2.6	1.5	2.9	1.2	2.5	1.7	1.3	1.6
Se	0.4	0.5	0.4	0.4	0.4	0.4	0.4	0.4	0.5	0.4	0.4	0.4	0.4	0.4	0.4	0.4	0.4
Br	7	7.7	9.1	7	6.3	13.3	10.9	6.4	7.6	8.4	6.2	5.6	7.9	8.1	8.4	6.8	7.6
Rb	9.8	11.4	9.1	10.5	8.6	8.5	12	9.5	10.3	10.1	9.5	9	9.4	12.7	12.2	11.3	10.1
Sr	488.2	506.1	549.8	407.2	480.5	553.9	466.9	550.5	485	480.5	490.6	484.2	441.8	488.5	527	456.7	444.5
Y	5	5	4.6	4.8	4.9	5	6.6	5.1	5	4.9	5.7	5.9	5.3	5.6	6	5.5	5.7
Zr	53.5	55.9	87.4	43.3	57.4	84.3	39.1	58	61.1	63.6	53.2	58.9	42	69.8	89.8	61.9	49
Nb	2.6	2.6	4.2	4.3	2.6	3	2.8	4.1	2.8	2.4	2.9	3.3	2.9	3.6	3.7	3.2	3.1
Mo	2.8	2.5	3	4.2	3.7	3	2.7	2.9	2.9	2.6	3	3.3	3	3.5	6.2	3.4	1.8
Cd	0.5	0.4	1	0.5	0.9	1.7	0.9	0.9	0.9	0.9	1.1	1.7	0.9	2.6	0.6	0.7	0.7
In	1	0.9	1.1	0.9	0.8	1.1	1	1	1	0.9	1.1	1.2	0.9	1.1	1.3	1.1	0.8

Table C.2. Elemental Compositions (ppm)

Element	87b	84b	80b	7a	79	78	74a	70a	6a	65a	63c	61b	61a	5a	59b	57a	52
Co	9.1	11.3	9.1	9.7	16.9	18.3	15.4	10.4	10.8	15	14.5	9.4	7.3	14.6	18	13.2	8.3
Ni	9.6	8.9	10.1	12.8	10.4	5.9	4.4	4.4	8	8.7	10.3	12.3	5	16.8	6.8	6.2	9.7
Cu	38.6	50.6	61.8	78.3	29.2	4.7	17.1	2.2	55.2	50	50.9	60.5	3.6	55.5	4.7	2.3	61.2
Zn	11.7	10.5	10.6	11.9	12.8	6.3	5.6	3.5	9.5	12.7	13.5	12.2	7.3	16.9	6.6	5.5	11.6
Ga	4.2	2.1	3.1	1.9	2.6	4.5	3.4	4	3.3	3.9	3.9	4.7	3.8	1.6	4.1	3.8	2.7
Ger	0.7	0.6	0.5	0.9	0.6	0.5	0.6	0.8	0.6	0.6	0.6	0.7	1.2	0.6	1.3	0.7	0.5
As	1.4	2	3.3	2.4	1.6	0.9	1.8	1.1	1.4	1.9	1.3	2.1	1.7	2.6	1.5	1.8	2.6
Se	0.5	0.4	0.4	0.4	0.4	0.4	0.4	0.4	0.4	0.4	0.4	0.5	0.4	0.4	0.4	0.4	0.4
Br	6.3	8.9	6.1	6.7	10.4	12.2	10.8	4.6	7	6.4	6.7	7.5	6.1	9.9	10.8	10.5	7.9
Rb	10.4	10.8	9.9	9.8	9	13.3	15.8	14.1	9.7	10.2	10.3	10.8	11	7.6	11.4	12.9	10.8
Sr	534.9	508.3	463.9	510.6	518.1	473.7	524.9	436.5	482.6	508.6	510.5	549.4	499.6	564.1	424	456.1	489.6
Y	7	6.1	4.7	6	4.6	4.9	5.4	5.1	5.4	5.5	5.5	6.8	5.5	5.4	5.5	6.2	6.1
Zr	56.8	69.7	49	55.8	80.6	52.4	39	48.6	55.4	49	52.9	62.1	45.6	69.4	55.9	61.7	51
Nb	4.4	7.8	2.5	3.5	4.8	3	2.6	3.6	4.2	4.3	3	3.8	3.6	2.4	2.6	2.8	2.8
Mo	3.1	6.7	4.2	3.1	3.3	3	5.7	3.6	6.1	2.8	5.2	3.7	4.4	3.3	2.5	2.7	3.1
Cd	1	0.8	0.9	1	0.8	0.9	0.9	1	1	0.9	0.9	1.7	0.8	0.9	0.8	1	0.8
In	1	1	1	1	0.9	1	0.9	1.5	1.1	0.9	0.9	2.7	0.8	0.7	0.8	1	0.4

Table C.3. Elemental Compositions (ppm)																	
Element	4a	46	43b	3a	39	38a	33	32	2a	29	28	19b	16b	16a	15b	14a	12a
Sn	13.4	16.4	11	1.1	12	18	1	9.4	18.1	13.1	11.5	8.2	1.1	5.5	8.7	4.1	2.9
Sb	14.8	18.1	132	1.1	16.8	119.4	1.2	12.7	15.2	30.7	5.4	10.1	1.2	3.8	20.3	5.1	4
Te	1.5	1.5	1.6	2	1.5	2.6	1.6	1.5	2	0.7	1.9	2	1.6	1.7	2	1.8	1.2
I	2.9	2.8	2.9	3.2	2.7	2.8	3	2.8	3.3	2.6	3.6	3.5	2.9	3	3.5	2.8	2.2
Cs	4.9	6.2	5	4.6	4.6	4.8	5.4	4.8	4.9	4.5	6.3	6.2	11	5.2	6.1	5.5	3.8
Ba	293.2	323.4	314.2	261.7	292.1	337.3	302.1	289	328	301.8	304.5	304.6	293.4	296.3	312.6	313.5	286.8
La	19.5	9.2	24.5	10	13.1	19.6	11	14.1	10	18.1	14	19.6	27.9	15.2	18.6	11	7.7
Ce	14	20.5	37.7	14	30.6	24.5	31.2	14	36.6	28.1	37	31	15	21.8	18	29.2	19.5
Hf	6.5	5.7	6	3	6.5	5.3	3.9	6.4	6.9	8.6	7.6	5.1	3.5	5.9	3.8	4.4	4.1
Ta	7.6	6.8	4.9	3	6.5	7.2	3.2	7.2	7	6.9	6.8	6.1	3.2	5.1	5.7	5.3	5
W	3	3.4	2.9	2.7	2.9	3.1	3.5	3.2	3.1	3	3.4	3.3	3	3.2	3.5	3.1	2.9
Hg	1	0.5	1.1	1	0.9	1.1	1	1.1	1	0.9	1.1	1	1	1	1.1	1	1
Tl	1.2	1.3	1.1	0.9	1.1	1.3	1	1.1	1.2	1.3	1.2	1.2	0.9	1.2	1.1	1.1	1
Pb	150.9	146.5	63.1	13.3	102.6	158.8	6.8	64.8	119.2	162.1	91.8	64.2	9.6	63.2	86.6	55	59
Bi	0.7	1.3	1	0.9	0.6	1.3	0.8	1	1.2	1.3	1.2	1.1	0.8	1.1	1.1	1	0.9
Th	0.7	0.7	1.2	0.8	0.5	1.1	0.9	1	1.7	1	1.1	1	0.9	0.8	1.6	0.7	0.8
U	13	6.3	12.9	5.9	6.4	15.4	6.1	5.6	6	5.5	8.7	16.5	6.3	18.3	18.7	14.8	6.4

Table C.4. Elemental Compositions (ppm)

Element	87b	84b	80b	7a	79	78	74a	70a	6a	65a	63c	61b	61a	5a	59b	57a	52
Sn	3.8	19.3	3.9	9.8	8	1.1	4.4	1.6	5.4	5.4	5.4	6.4	0.7	13.4	0.7	1.2	20.9
Sb	3.8	14.7	27.8	8.6	52.3	1.2	3	0.9	16.2	4.2	5.1	5	1	69	1	1.2	15.1
Te	1.8	1.5	1.4	1.7	1.4	1.6	1.6	2.3	1.7	1.6	1.5	2	1.4	1.6	1.5	1.3	1.3
I	3.1	2.7	2.6	3	2.5	2.9	2.3	5.1	3.1	5.3	2.8	3.5	2.4	2.9	2.6	2.8	2.4
Cs	5.4	4.6	4.7	4.5	6.5	5.1	4.3	7.5	5.5	11.7	7.5	6.3	4.3	4.2	4.7	5.6	7.5
Ba	287.9	293.8	359.9	319.7	260.2	281.9	321.6	282.8	315.8	321.7	310.3	328.4	304.5	306.9	277.9	293.1	301.5
La	16	13.1	16.4	14.1	22.3	14.7	12.9	16	17.9	10	15.6	14.6	17	16	20.9	20.2	19.4
Ce	25.1	34	26.8	36.9	27.3	20.3	23.7	22	33.2	29.2	28.9	33	24.2	19	38	30.4	16.5
Hf	5	5.8	5.3	7.3	5.2	2.8	3.6	3.6	5.2	6.1	6	5.7	3	6.3	2	3.4	8.6
Ta	6.1	6.2	6.7	7.5	4.9	3.1	4.1	3.1	6.4	6.3	6.2	7.2	3	6.4	3.1	3.1	6.5
W	3.8	3	3	3.3	2.8	3.2	2.9	3.4	3.4	3	3.1	3.6	2.9	3.2	2.8	2.9	2.8
Hg	1.1	1	1	1.1	0.9	1.1	0.9	0.9	1	1.1	1	1.1	1	0.9	0.9	1.1	1
Tl	1.2	0.9	1.2	1.3	1.1	1	1	0.9	0.5	1.2	1.2	1.3	0.6	1.3	0.9	0.9	1.3
Pb	63.6	157.1	109.4	128.5	72.5	30.9	41.1	6.3	85.3	80.9	82.8	84.1	14.8	156.2	7.6	9.2	174.4
Bi	1.2	1.3	1.2	1.2	1	0.9	0.9	0.9	1.1	1.1	1.1	1.1	0.8	1.3	0.8	0.9	1.3
Th	1.7	1	1.2	1.5	1	0.7	1.3	0.7	2.2	0.8	1.2	1.8	0.9	0.9	0.6	1.6	1.1
U	7.2	7.4	6.1	5.9	5.3	6.4	6	7.2	6.6	6.3	6.7	7.9	5.7	8.1	7.6	9.8	7.3